SOLAR ENERGY
JOURNAL OF SOLAR ENERGY SCIENCE AND ENGINEERING

VOLUME II | APRIL, 1958 | NUMBER 2

Table of Contents

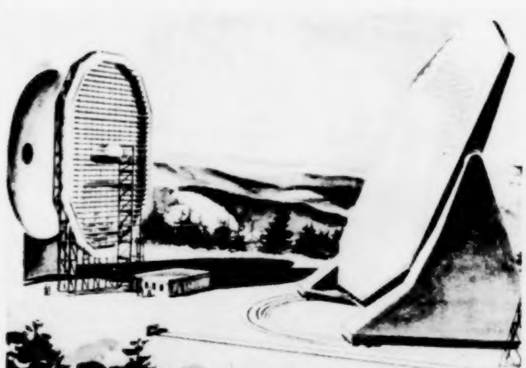

The cover for this issue shows an artist's sketch of the giant solar furnace which will be built for the Air Force near Holloman Air Force Base, N.M. The furnace, developed jointly by J. W. Fecker, Inc., and Pittsburgh-Des Moines Steel, will consist of a 145-ft square, 1½ million-lb heliostat (left) and a 108-ft diameter parabolic mirror (right). This latter will focus the sun's rays onto a 5-in. diameter spot in the laboratory unit in front of the venetian-blind-like shutter. Temperatures of 7,000°C are expected.

SOLAR ENERGY RESEARCH: PROGRAM IN THE NEW DESERT RESEARCH INSTITUTE IN BEERSHEBA*

By H. TABOR

The National Physical Laboratory of Israel, Jerusalem

Research in thermal processes for harnessing sunshine, leading to work on selective black surfaces of low emissivity, is described. With the resultant low radiation losses, the convection losses become dominant, and these have been reduced in a new collector by mounting the solar receiver horizontally face downwards. A low-concentration stationary mirror directs the sunshine upwards. Steam for industrial use is the target, and a pilot plant installation is now being designed. Other problems being studied include new flat-plate collectors for water and air heating, a small turbine operated by a heavy vapor, and heat storage.

Solar air conditioning is being considered from two approaches, one being the use of absorption-type water chillers operated with solar heat, the other using the Altenkirch system of designing a house as a cyclic absorption dehumidifier.

BACKGROUND

Some two and a half years ago solar energy exploitation research was started in this laboratory. The work was confined entirely to thermal systems, as these appeared to offer the best chance of early utilization at a reasonable conversion efficiency. Photochemical and photoelectric systems have not so far been studied, as it was felt that these were long-term solutions, dependent upon a great deal of basic research.

In studying the thermal systems, it was known that in the production of low-temperature heat, i.e., heat at temperatures not far removed from ambient temperature, quite high efficiencies could be obtained with relatively simple collectors. As a consequence, simple solar collectors have been used experimentally as heat sources for heat pump installations for house heating in the United States. However, as the temperature of collection is raised, the efficiency of collection falls, resulting in larger collectors being necessary and a corresponding drop in the economic value of solar heat. As an alternative to larger collectors operating at low efficiencies, mirror systems have been used to provide optical concentration. These could reach higher temperatures, but were usually expensive because of the need to track the apparent motion of the sun.

The decrease in efficiency with rising temperature is due to the increase in heat losses from the blackened receiving plates or tubes used, and a few historical attempts are recorded at reducing these losses. Several workers proposed evacuated glass envelopes to surround the energy-absorbing surfaces. The study showed that this procedure could, at best, result in only a slight improvement, for the major source of heat loss from the heated surface (if protected from wind by a glass or other cover) is thermal radiation and not convection, and that an effective reduction of heat losses would occur only if the radiation losses were reduced.

This study led to the development, in this laboratory, of the theory and principles of selective radiation, a scientific basis for reducing radiation losses from black surfaces used as solar energy absorbers.

Because solar energy absorbers are necessarily black, it had been accepted as an inevitable fact that such absorbers would act substantially as blackbody radiators, i.e., that they would have high thermal emissivity, which indeed they invariably had. However, it was shown that this was not necessarily so. Because solar radiation as received at the earth is confined to wavelengths in the range 0.3-2.5 μ, whereas the heat radiated from bodies at temperatures up to a few hundred degrees C is of much longer wavelength, it is possible to produce surfaces which, like optical filters, have different optical properties at different wavelengths. Thus, highly polished metal surfaces usually have very low emissivity, i.e., are good reflectors of longwave heat radiation. If these surfaces can be blackened, for the visible spectrum, in such a way as not to affect their characteristics to long waves, then a selective surface is obtained which may be a good absorber for sunlight and yet a poor emitter of heat.

Such surfaces were prepared in this laboratory and incorporated into solar collectors of otherwise conventional design. A great improvement was shown, particularly for applications where higher temperatures were required. Thus, a flat-plate collector normally suitable only for the heating of water was found to be able to produce steam at atmospheric pressure with a daily efficiency of about 30 per cent.

For the last two years, work has proceeded on the methods of producing selective black surfaces on large areas

*Lecture delivered at the opening of the Arid Zone Research Institute in Beersheba, Israel, on October 30, 1957.

and at low cost. A number of difficulties have been overcome. In the first place, because the selective surface *is* a surface, it must be highly stable to the effects of heating and exposure to the atmosphere. Secondly, surfaces produced by such techniques as vacuum deposition had to be ruled out as being too expensive for large areas of massive plates.* This has led to the use of nickel-plated surfaces or lightly anodised aluminum as the base metal — since these are inherently stable surfaces — coated with a very thin selective black coating produced either by chemical or electrochemical deposition. Recently galvanized iron has been introduced as a suitable base metal (for low-temperature applications such as water heaters), since it is known that in less advanced countries this material is more readily available and local craftsmen are accustomed to its use. From a thermal point of view, it is, of course, inferior to aluminum. The blackening of the galvanized iron is simple, involving a dip in a preparatory bath followed by electrolytic deposition from a bath producing a nickel-zinc sulphide complex.

To date, stable selective surfaces have been produced with absorptivities to sunlight of about 90 per cent and emissivities in the region of 8-12 per cent that of a perfect blackbody radiator.

PRESENT AND FUTURE PROGRAM

The program is divided into two main parts; predominantly applied research and predominantly pure research. We will deal with the former first, as this is the one of major interest to the Beersheba Institute.

Applied Research

Much of this program is designed to exploit to the full the possibilities opened up by the use of selective surfaces.

Heat Flow

A good deal of work has been done on heat flow, in particular with a view to raising collector efficiency. For example, it has been shown that the conventional box used for solar collectors can result in unexpected heat losses from the edges of the collector plate because, whilst care is usually given to provide an adequate degree of thermal insulation at the rear of the plate, the energy loss from the edges is not appreciated. Thus, in electrostatic field theory a charged plate has the greatest concentration of charge at the edges and corners. A similar state of affairs exists in a thermal field. This has led to the design of a new type of box in which the insulation at the edges of the plate is as thick as that at the rear face. This allows less insulation to be used at the rear for the same heat loss, leading to improved economics. The full theory is described in a paper about to be published. In constructing the new box, opportunity was taken to use asbestos cement molded to the required shape instead of the present wooden boxes with their galvanized iron flashing incorporated to improve the weathering.

Because the radiation losses from collectors can be reduced by a factor of 8-10 using selective surfaces, we find that the obstacle to further improvement is now the convection loss. As an example, in a flat-plate solar water heater of conventional design, the heat losses are divided approximately in the ratio: radiation 60 per cent, convection 30 per cent, and rear and edge losses 10 per cent. If the radiation loss is reduced by a factor of 10, the total losses are now 46 per cent of their former value, the major term now being convection loss. If by any means the latter could be reduced by a factor of say 5, the total losses would become 22 per cent of the original value or an improvement factor of nearly 5.

Consequently, research has been conducted on the elimination or reduction of convection losses in solar collectors. Some experiments on evacuated collectors have been conducted, but were discontinued on account of technical difficulties when dealing with vacuum over large areas.

An extremely simple method of reducing convection loss to a very small value has been introduced and is now the subject of patent applications. It comprises mounting

*Vacuum deposition of large areas on plastic sheets is now a relatively cheap commercial process because the thin flexible sheets used are rolled up inside the vacuum chamber. If a continuous "roll" process is not possible the method is very expensive.

TABLE I

COMPUTED REDUCTION OF HEAT LOSSES BY USE OF A SELECTIVE BLACK RECEIVER PLATE AND AN INVERTED COLLECTOR

Plate temperature 150°C
Glass-cover temperature 40°C
6 cm of good insulation on rear

	Normal black (emissivity 0.95)		Selective black (emissivity 0.95)	
Horizontal facing upwards	Radiation Loss**	920	Radiation loss	109
	Convection loss	406	Convection loss	406
	Rear loss	100	Rear loss	100
	Total	1426 = 100%	Total	615 = 43%
			Improvement factor 2.3	
Horizontal facing downwards (inverted)	Radiation loss	920	Radiation loss	109
	Convection loss	73	Convection loss	73
	Rear loss	100	Rear loss	100
	Total	1093 = 77%	Total	282 = 20%
	Improvement factor 1.3		Improvement factor 5.0	

**Losses are in kcals/sq m, hr

Observe how inversion with a normal black results in only a small improvement, but with a selective black the total improvement is a factor of five.

a flat-plate collector in a horizontal position facing *downwards.* It is known that heat transfer in air between parallel horizontal planes when the heated plate is uppermost is almost entirely by conduction through the air and not by convection. The heat transfer is thus only a fraction of that occurring in a collector facing upwards. Coupled with the use of a selective black for low radiation transfer, the net result is a collector with about 1/5 the heat losses of a conventional collector. (See Table I.)

Of course, because the collector faces downwards the sunshine must be reflected onto it by means of a mirror, but the clue to the situation is that this mirror need have very little concentration and therefore need not be very accurate nor be heliostatically mounted. Thus a model is demonstrated on the campus here in which the mirror provides a concentration of about 4 and is fixed, the tilt being manually adjusted about once a week. Because of the very low heat losses the system is comparable to conventional mirror systems with an optical concentration factor of the order of 20.

New Collectors

A number of new collectors is being designed and tested. The water heater which has been sold for some years in this country has been compared with a new collector designed in this laboratory, with the latter showing nearly 100 per cent improvement. Thus, the present two collector panels recommended for a normal family can be replaced by a single panel, saving money for the customer and raw materials for the country.

Methods of making solar roofs, i.e., flat-plate collectors of large area, are now being studied with particular reference to local conditions. Several such roofs will be erected on this campus.

The production of steam for industrial purposes is now considered feasible, and the first pilot plant to yield 1-2 tons of steam a day at pressures of 6-8 atmospheres will be built in Beersheba for a local chemical works.

The plant will be a rather more elegant version of the steam generator on the campus here but will use the same basic principles of reduced heat losses and a moderate concentration mirror. First estimates are that the steam produced with the solar boiler may be less expensive than that produced by fuel at the same factory.

Solar air heaters are also being studied for possible use for agricultural purposes.

Finally, the thermodynamics of heat collected in solar ponds is also being studied with a view to determining the possibilities of very large collectors for the operation of temperature-difference power units and water distillers.

Solar Engines

Improved collectors reopen the question of power from solar energy, particularly for small units of 1-10 hp. Such units could satisfy an important need in many arid regions of the world. A start has been made in the study of a turbine specially designed for this purpose. It may be shown that, if a working fluid other than steam is employed, many of the objections to small steam turbines are overcome, and the result is rather attractive. Unfortunately, the design and construction of the first prototype is very costly and will depend upon suitable financial support being forthcoming.

Heat Storage

A number of systems of heat storage are being considered. However, much of this work is concerned with basic physical chemistry and forms part of the "pure" research program.

Air Conditioning and Cooling

Much experimental work has been done in the United States on heating of buildings with solar energy, a system which involves the contradiction of large demand at times of poor supply. Solar cooling is, from this point of view, far more attractive and of perhaps greater interest in Israel and other sunny countries.

The present program envisages the use of absorption-type chillers operated by hot water or low pressure steam from solar roof collectors. One serious problem is the discharge of rejected heat which is much greater (of the order of 2½ times) in such a system than in a compressor-type cooling system. Water-cooling towers may consume more water than we can really afford for this purpose. However, if house cooling is considered essential for comfort and working efficiency in hot regions, then some form of artificial cooling is required. As electrically operated air conditioners operate during peak load hours of the electrical network of Israel, the solar operated coolers, even if superficially more expensive, may turn out to be cheaper when the extra installed kilowatts of the central power stations are taken into account.

Consideration is also being given to the methods of cooling a building with the aid of solar energy proposed by the late Dr. Altenkirch.* One of his proposals involves constructing a simple dwelling in the form of a cyclic absorption dehumidifier. There are no mechanical or electrical devices involved; the walls contain the dehumidifying agent, and the sun itself sets off the cycles of operation. Being based on dehumidification (but without temperature rise), the system is not too suitable for very dry regions, and a slightly more complicated system is suggested. After the full analysis is completed a decision will be taken on whether to construct some experimental buildings using these techniques.

Effect of the Desert

One major factor in solar devices is the expected life of the apparatus, for upon this depends the rate at which the high initial cost can be amortized. It is proposed to use this scientific institute in Beersheba, set on the edge of the Negev Desert, to study the effect of local climate, sandstorms, etc, on the performance of mirrors, glasses, and other materials used in constructing solar collectors. The information gained should be of considerable value to other arid areas with similar climates.

*See, for example, the book *Die Absorptionskaltemaschine* by J. H. Dannies (Bruck Verlog Kurt Schmersow, Hanover 1951), p. 160, or Altenkirch's contributions to Institut International de Froid, 1934, or E. Altenkirch, *Zeits fur die gesammte Kalte Industrie* 6:1-6, June, 1937.

Solar Incidence Recording

It is proposed to set up here recording instruments for the measurement of solar radiation on horizontal and tilted surfaces, both direct and diffuse. Apart from providing useful design data, the figures are needed to compute collection efficiencies of collectors being tested on this campus.

• • •

Pure Research

To complete the picture we sketch the programme of pure research, although it will not be carried out here in Beersheba, but in the Laboratory's facilities in Jerusalem. At present, the pure research is concerned with the optical mechanism of selective surfaces. Subject to funds being available, we hope to inaugurate basic research on three other subjects related to solar energy. These are in the fields of photoelectric phenomena, the physical chemistry of heat storage, and the theory of fuel cells. The latter, whilst not directly connected with solar energy, is closely related to the question of energy utilization.

THE COMBINATION OF LOCAL SOURCES OF ENERGY FOR ISOLATED COMMUNITIES

By E. W. GOLDING

Electrical Research Association, London, England

This article emphasizes the importance of a supply of energy for the improvement of living conditions in, and general development of, underdeveloped areas. The costs of importing energy, whether in electrical form or as fuels, is usually expensive for such areas because of their remoteness from bulk supplies with consequent high costs for transport. It is suggested that, to supply power to isolated communities scattered over a wide area and with a consequent low density of population, local sources of energy should be used. The most widely distributed local resources are wind, solar radiation, and organic waste materials. The methods of using these by means of equipment now under development are described, and the probable costs involved are also estimated. As a conclusion, the article outlines a possible scheme for the combination of local energy resources to supply all the energy needs of a community in an underdeveloped area.

In this present age, when problems of the supply of energy in one form or another have become so universal, it is not surprising that the underdeveloped areas of the world should become conscious of their needs for energy to take them along the road already followed so successfully by the more industrialized countries. Whatever the divergence of views on methods of power production, one fact clearly emerges — the availability of power and the standard of living are closely connected. Indeed, there is a rough proportionality between annual income, expressed not just in monetary terms but in indexes of material prosperity, and the consumption of energy per head of population. Several recent international conferences have shown that the less developed countries recognize this truth. The latest, the sectional meeting of the World Power Conference in Belgrade this summer, had as its theme "Power as a factor of development of underdeveloped countries."

The position is, then, that the need for energy as an aid to development is fully appreciated, but methods of supplying this energy economically are not yet decided.

What are the possibilities?

To attempt an answer to this question one must first consider the areas concerned and the purposes for which, in the initial stages of development, they may need energy. No precise definition for an "underdeveloped" country can be given to satisfy everyone, but it is generally accepted that underdeveloped countries are poor economically and contribute less than their proportionate share towards the world's production of food and other commodities essential to the well-being of the rapidly growing population. There are, of course, vast areas in the arctic and antarctic zones which must be so classified and some in the temperate zones. But the areas which are important, particularly because they are inhabited by about half the world's population — in Asia, Africa, and South America — lie in the tropics and subtropics. Some examples of the annual per capita consumption of electrical energy (taken as representative of the more general consumption of energy of all kinds) are given in Table I.

TABLE I

PER CAPITA CONSUMPTION OF ELECTRICAL ENERGY

Area	Annual consumption of electrical energy, per head of population (kwh)
Central America and the Caribbean	207
Oceania	180
South America	175
Asia (Middle East)	54
Africa (excluding Union of S. Africa)	48
Asia, Far East (excluding Japan)	27

The average values of annual consumption per head given in the table must be compared with 4,200 kwh in U.S.A., 5,400 kwh in Canada, 6,800 kwh in Norway, at the upper end of the world scale, and between 1,000 and 2,000 kwh for the group of industrialized countries in Western Europe.

The relevant facts, from the point of view of energy supplies, are as follows:

(i) The trend of development, at present or in the near future, in most of the underdeveloped areas will be for agriculture and rural industries. The existence of minerals or valuable resources other than cultivable lands might justify heavy expenditure on development quite beyond what would be economic for the majority of the areas, but such favourable circumstances should be considered as exceptional.

(ii) The population, though large in total, is usually scattered so that its density is low. Villages or agricultural communities are often small; they are almost nonexistent in many large stretches of territory, e.g., in the Middle East, where the people follow a nomadic way of life, mov-

ing about with their flocks and herds and continually seeking pastures.

(iii) The present demand for power by the inhabitants is almost nonexistent if only because of their ignorance of the possibilities. Instruction in the use of mechanical forms of power to augment or replace the commonly used, but inadequate, animal power will be essential. But, for some time to come, the quantity of energy needed at any one place will be small. "Load centres," as they are known in the advanced countries, are unlikely to arise quickly.

(iv) The areas are very often remote from power stations or networks and from bulk supplies of fuel for power generation. Railways and good roads are frequently lacking, so that transport is difficult and expensive.

(v) Low levels of income and national finances generally preclude the establishment of power systems on the lines followed in indùstrialized areas.

(vi) Though the inhabitants are often by no means unintelligent and possess innate ability to master modern techniques, education, particularly in technical matters, is essential if development is to make progress.

The main conclusion to be drawn from these facts is that the real problem to be faced is that of supplying energy, at an economic cost, to thinly populated areas without any well-defined load centres, at considerable distances from power networks and to peoples without experience of the use of such energy. Clearly this problem has two parts. The first is concerned with the means of providing the energy and the second with planning the load system and instructing the inhabitants in its use to take full advantage of the service provided.

Let us consider these two parts in turn.

MEANS OF SUPPLYING THE ENERGY

There are two obvious alternatives: (a) the energy can be imported into the area where it is needed, or (b) it can be derived from energy sources which may exist on the spot.

(a) Imported Energy

Again, there are two choices: electrical energy can be transmitted to the area from the nearest power network, or fuel — usually diesel oil — can be brought in by surface transport for use in generating stations located at central points in the area. For relatively small supplies of energy, as the following figures show, both of these alternatives result in high costs per kilowatt-hour.

For a power demand of 500 to 1000 kw and distances of 100 to 300 miles, the present cost of electrical transmission lines varies from about £1600 to £2100* per mile according to the transmission voltage (11 or 33 kv) and cross section of conductor used. An annual return of 15 per cent of the capital cost of the line is needed for economy, so that, on the assumption of an annual load factor of 30 per cent, the transmission costs per kilowatt-hour consumed can be derived as in the following table.

TABLE II
Costs of Electrical Transmission

Maximum power demand	Trans-mission distance (miles)	Capital cost of line (£)	Annual capital charges (£)	Annual energy supplied (kwh)	Transmission cost per kwh (pence)
500 kw	100	160,000	24,000	1.3×10^6	4.4
	300	555,000	83,300	1.3×10^6	15.4
1000 kw	100	160,000	24,000	2.6×10^6	2.2
	300	624,000	93,600	2.6×10^6	8.6

If a distribution cost of about 1d per kwh — which would not be excessive for a thinly populated area of the kind being considered — is added to the transmission cost, the total charge per kwh will range from 3.2d (for 1000 kw and 100 miles) to 16.4d (for 500 kw and 300 miles), plus the initial cost of the energy at the sending station.

Now consider, instead ,diesel power generation at small central stations in the area. At many up-country places distant from a railhead, diesel fuel costs up to 48d per gal. Taking a figure of 36d per gal, the fuel cost per kwh generated would be 3d. Adding capital and maintenance charges (with 30 per cent load factor) and 1d per kwh for local distribution, the total cost would be about 5.3d per kwh for 1000 kw demand and 6d per kwh for 500 kw. In obtaining these figures, no account has been taken of the possibility, if not indeed probability, that maintenance costs for diesel plant in such areas may be abnormally high.

To summarize, whether energy is imported in electrical form or as diesel fuel, the price to the consumer (under the conditions of load and distance specified) cannot be less than 4d per kwh and may be as much as 17d per kwh.

(b) Local Sources of Energy

These sources may be:
wind
solar radiation
water power
vegetable wastes
animal power (consuming locally produced fodder)

Various combinations of these resources can be envisaged according to the particular district considered. All of them have characteristics, as power sources, which call for treatment different from that for the more conventional methods of producing energy.

Wind and solar radiation can be classed together. Both are freely available and inexhaustible but have the disadvantages of being random in nature and, because of their dilute form, requiring rather large and potentially expensive plants to harness them. They must, therefore, be fully utilized whenever they become available, unless the capital charges on the plant are to remain unrewarded by useful output.

Small water power schemes would be possible in some places but have the disadvantage, even if they can be cheaply installed, of being fixed in location and, as a corollary, involving high costs for distribution of their energy production. Waste vegetable matter in the forms of sisal waste, bagasse, rice husks, straw, coconut wastes, tree lop-

*Editor's Note: The author's figures in English monetary units have been retained. These may be approximately converted to U.S. currency as follows:
1 pound (£) = 20 shillings (s)
= 240 pence (d)
= $2.80 (U.S.)

pings, etc., can often be found. In dry areas, however — and many underdeveloped areas happen to be arid or semiarid — great care must be taken to avoid using up any vegetative cover which assists the growth of herbage by providing shade or which prevents soil erosion.

Animal power is very commonly used in these areas, but, apart from the 10 to 15 tons of fodder which each animal consumes per annum, the cost of the animals, their short working life, the low power output, and the need for men to drive them lead to an energy cost of 6d to 12d per kwh. In spite of its apparent convenience, animal power is not cheap.

ESTIMATED COSTS OF ENERGY PRODUCED FROM LOCAL RESOURCES

The energy sources with the widest distribution, and therefore most worthy of consideration when their combination to provide a community service is envisaged, are wind, solar radiation, and organic materials. Of these, perhaps wind power is the most advanced in development, but reasonable estimates of energy costs from the other two can be made as an indication of their order of magnitude.

(a) Wind-Driven Machines

These are of two kinds, (a) nonelectric, mainly used for water pumping, and (b) electric, for more general purposes.

FIG. 1 — An 8 to 10 kw Allgaier wind-driven generator. This machine has a 6-kw alternator with a 2-kw exciter. The exciter can provide direct current for battery charging.

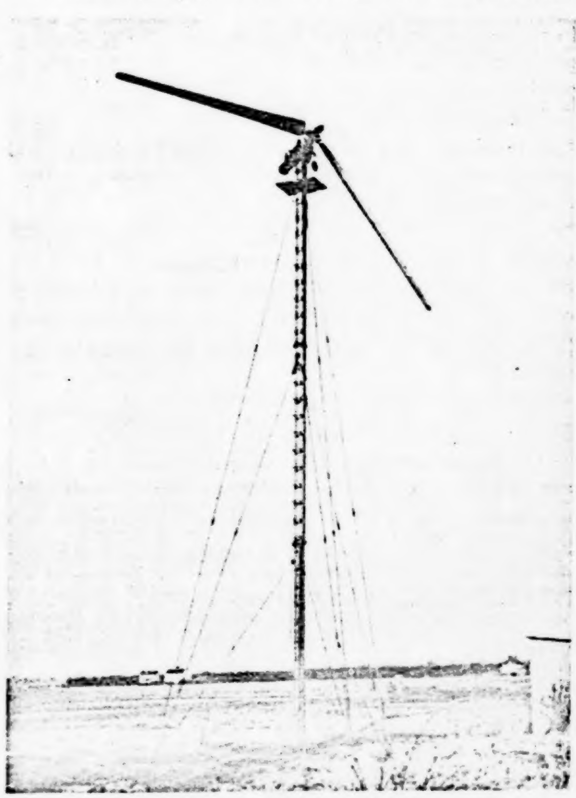

Water-pumping windmills are commonly used in dry areas, as well as in countries better supplied with water. They are designed to start pumping in low wind speeds of about 6 to 8 mph and to give full output at about 20 mph. Their installed cost varies, according to size, from about £150 for 6 ft diameter up to £500 for a diameter of 18 ft.

Wind-driven electric generators in sizes greater than that of the familiar small machines of 1-kw capacity or less, used for individual premises, are still under development but have advanced far enough for an estimate of their probable capital cost to be made. Thus, machines in the capacity range 10 to 50 kw or thereabouts will cost between £100 per kw to £200 per kw according to their rated wind speed (i.e., the minimum wind speed for full power output). The power in the wind is given by the formula

$$P(\text{in kw}) = 0.000005\, AV^3$$

where A is the area in sq ft swept by the rotor, and V is the wind speed in miles per hour. Obviously the higher the rated wind speed (V) chosen in the design the smaller will be the swept area (A) for a given rated power output, and the lower the capital cost. On the other hand, a high rated wind speed means a relatively low specific output (expressed in kwh per annum per kw) with a given wind régime. The shape of the wind régime curve (i.e., the velocity duration curve) is well enough established for the specific output to be given, in terms of the annual average wind speed at the site, for various values of rated wind speed. In the following table, values of specific output are given for two rated wind speeds together with energy costs on the basis of total annual charges, for interest, depreciation, and maintenance, of 10 per cent.

TABLE III

COSTS OF WIND-GENERATED ENERGY

Annual average wind speed (mph)	Rated wind speed 15 mph		Rated wind speed 25 mph	
	kwh per annum per kw	Energy cost in pence/kwh	kwh per annum per kw	Energy cost in pence/kwh
10	3,380	2.37	880	3.27
12.5	4,200	1.91	1,750	1.64
15	5,280	1.51	2,680	1.07
17.5	6,000	1.33	3,450	0.84
20	6,740	1.19	4,220	0.68

From these figures it is clear that when the annual average wind speed at a site is of the order of 15 mph or over, a rated wind speed of 25 mph will give cheaper energy than one of 15 mph, but the latter will be better for less windy sites.

In stating these energy costs it is implied, of course, that all the energy generated will be effectively used. It becomes *available* as the wind speed rises and, if it cannot be used at that time, it must either be stored or allowed to go to waste. The storage of energy is always expensive if some special device, e.g., an electric battery, has to be provided for that purpose alone. In fact, to attempt the "firming" of even one-quarter of the total power output by a battery may double the over-all cost of the energy. On the other hand, the annual charges on the plant are the same whether the energy is used or not, so that it is obviously uneconomical to allow energy to go to waste.

FIG. 2 — The Indian solar cooker is shown to an interested group at Burao, Somaliland Protectorate.

The answer to this problem is, surely, to arrange to use the energy as it becomes available, without storage except in so far as this may be inherent in the load itself, e.g., in water heating, water pumping, refrigeration, or distillation.

An almost universal requirement in any power scheme will be provision for electric lighting, and this must be given first priority, so that some storage of energy in a battery may be essential. This battery should, however, be limited in size — and in cost — to the minimum needed for the purpose.

Referring again to Table III, the importance of selecting favourable sites for the installations can be appreciated from the fall in the cost of energy as the annual average wind speed increases. Often there is a difference of 1 or 2 mph between the average speeds at points fairly close together, especially if their exposures to prevailing winds are different.

(b) Solar Energy Equipment

All workers interested in the development of equipment to utilize solar energy realize the need to reduce its costs, and there is no doubt that this cost will fall as more progress is made in their investigations. It may, therefore, be a little unfair to take the present capital costs as indicative of those which will apply to practical use, but one cannot yet assume that these will be lower. For flat-plate collectors used for solar water heaters, stills, and for space heating, costs of £1 to £2.5 per sq ft have been given. Concentrating collectors must vary in cost according to their size and purpose; the Indian solar cooker has a market price of £5 for an area just under 10 sq ft. Solar engines are inevitably rather expensive, and the latest prices quoted for the solar water pumping equipment made in Italy are of the order of £300 to £500 per hp.

To estimate costs of energy produced by solar equipment, annual capital charges may be taken as 15 per cent, while the output of energy can be based on available values averaging 4 to 7 kwh per sq m per day. In this way one arrives at figures such as those in Table IV. Admittedly these are open to question, but they are probably of the right order of magnitude.

TABLE IV

COSTS OF ENERGY PRODUCED FROM SOLAR EQUIPMENT

Type of equipment	Application	Energy cost (pence/kwh)
Flat-plate collectors	Water heating, distillation, space heating, and air conditioning	1 to 3
Flat-plate or concentrating collector	Motive power (e.g. water pumping)	6 to 10
Concentrating collector	Cooking and steam raising	up to 1
Thermoelectric and photovoltaic	Special uses involving very small power	several 100

From these figures it can be concluded that the applications to heating in various forms show promise of being generally economic. For motive power the energy cost is perhaps rather high, but, on the other hand, in dry areas the supply of water is so important that high costs for its production may be justified.

(c) Organic Materials

Under this heading can be placed the direct use of wood, charcoal, and dry material for heating and cooking, and the less direct use for power production.

Small steam engines, together with boiler and furnace, in a portable form have been developed. One of these, for which the National Research Development Corporation has been responsible in Great Britain, can have a capacity of 2½ to 5 hp, and its cost, when produced in quantity, may be £50 to £70 per hp. The calorific value of a range of waste materials, such as bagasse, coconut shells, rice husks, and straw, is around 8,500 Btu per lb, and the consumption of the 2½ hp engine would be about 30 lb per hour.

Other methods are the use of combustible material in a gas producer, thus saving fuel in a dual-fuel engine and, alternatively, the fermentation of fresh materials, like animal manures or sisal wastes, to produce methane which can be burnt directly for heating or cooking or can be used as an engine fuel. Particularly in Germany and France, methane plants have been commonly installed on farms and research is being done, in East and West Africa, India, and other countries, to develop this means of producing power.

Energy costs can be estimated as follows:

TABLE V

COSTS OF ENERGY FROM ORGANIC MATERIALS

Material	Application	Energy cost (pence/kwh)
Wood	Heating and cooking	1 to 3
Charcoal	Heating and cooking	5 to 10
Waste materials	Motive power	2 to 4

THE COMBINATION OF ENERGY RESOURCES

To cater to the energy needs of a remote community entirely from local resources could well be economic provided that a scheme were properly planned to ensure that these resources were fully utilized for purposes to which they were suited. In dealing with random sources of

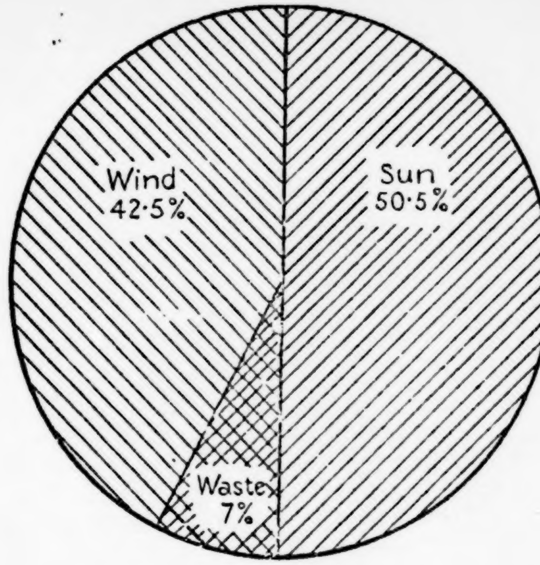

FIG. 3a — Division of the energy sources.

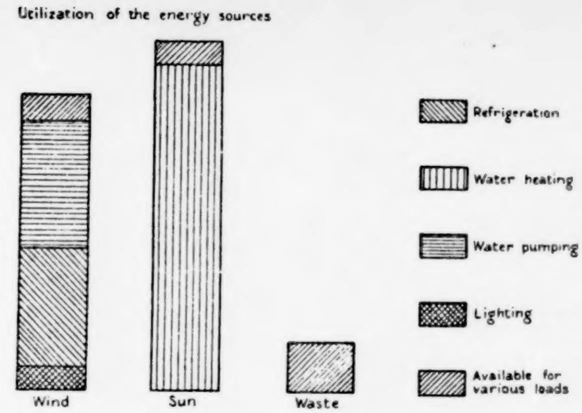

FIG. 3b — Utilization of the energy sources.

energy, when storage of energy is to be minimized because of its high cost, the characteristics — particularly the timing requirements — of the loads must be considered in conjunction with those of the various methods of power production employed. Thus, for example, water pumping for irrigation can be done at random times without any inconvenience, but cooking must be done when a meal is wanted and lighting is required only at night.

Recently the writer considered, in some detail, the possibility of supplying, as an experiment, a remote agricultural community with its energy needs for the development of about 100 acres of land as well as for domestic purposes. At the site concerned there was an annual average wind speed of 11.5 mph, annual solar radiation of about 195 kwh per sq ft of horizontal surface, and about 100 tons per annum of combustible waste material. The rainfall was 12 to 24 in. a year; the maximum daily temperature range was 78°F to 90°F and the minimum 48°F to 63°F. Underground water, at shallow depth, was available. Table VI gives an outline of the proposed method of supplying the annual energy needs through the provision of four 10-kw wind-driven electric generators, two water-pumping windmills, a solar pump, about 600 sq ft of solar collectors, and a 5 hp steam engine driven from waste material. A small electric battery is included to cover lighting and small essential loads when there may be calm weather so that no wind power is available. The costs of energy estimated include an allowance for

TABLE VI
POWER PLANT, LOAD DISTRIBUTION, AND COSTS FOR AN EXPERIMENTAL SCHEME

Type of equipment	Probable cost of energy (pence/kwh)	Load to be supplied	Timing requirements	Probable annual energy consumption (kwh)	Total annual cost of energy (£ sterling)	Notes
Wind-driven electric generators	2.2	Irrigation, pumping Agricultural loads Heating, lighting	Random Daytime Precise times (night)	65,000	600	Main source of power for irrigation and for lighting. Supplementing solar for heating.
Water-pumping windmills (nonelectric)	8	Water pumping for domestic supply	Random	3,000	100	Pumping in low wind speeds
Flat-plate solar collectors	0.85	Water heating, space heating, refrigeration, distillation	Random	56,500	200	Costs include provision for ancillary equipment.
Concentrating solar collectors	0.4	Cooking and steam raising	Precise times in the day	15,000	25	
Solar pumping engine	8.6	Water pumping and small miscellaneous power	Random	2,500	90	Used in conjunction with wind power plant.
Steam engine	6	Agricultural loads and stand-by power	Stand-by	10,000	250	Costs include ancillary equipment for stand-by purposes
Electric battery	—	Lighting and small essential loads	Precise times	—	200	Battery of small capacity to cover essential loads in calm weather.
TOTALS				152,000	£1,465	

Average cost per kwh = 2.31d

ancillary equipment, such as that for electrical distribution, control gear, water piping, load-selecting switches, etc.

The costs have been estimated as closely as possible, and, while in operating such a scheme there would doubtless be unforeseen items of cost, on the other hand it is quite possible that some of the proposed equipment could be omitted without great detriment. The division of the energy supply between the three sources, wind, solar radiation, and organic wastes, is shown in Fig. 3.

Experience with a scheme of this or similar kind is badly needed if any progress is to be made towards putting local energy resources to use.

The basis for the annual costs has been taken as 10 per cent charges for the wind power and steam plant, 15 per cent for the solar plant, and 20 per cent for the battery. It is interesting to note that the calculated over-all average cost of energy is only 2.31d per kwh, while an estimate for the same job to be done by diesel-electric plant, with fuel at 36d per gal, gave a figure of 3.8d per kwh.

VOL.
2
1958

A STUDY OF TEMPERATURE MEASUREMENT IN A SOLAR FURNACE

By BYRON B. BRENDEN, HERBERT W. NEWKIRK, JR., and SIDNEY H. WOODCOCK

Hanford Atomic Products Operation, General Electric Co., Richland, Washington

A survey indicates that thermocouples and two-color pyrometers can be used to measure accurately the temperature of a specimen being heated in a solar furnace. The thermocouples found to be most satisfactory and accurate to ± ¾ per cent in the range room temperature to 1100°C are chromel-constantan, chromel-alumel, useful in oxidizing atmospheres, Driver-Harris, No. 242 (Geminol P) vs. No. 33 (Geminol N), useful in neutral and reducing atmospheres. The range 1100°C to 3500°C can be determined by means of a two-color pyrometer with an accuracy of better than ± 10°C. Both instruments, if properly designed, have been demonstrated to be independent of the emissivity of the specimen and the environmental conditions existing in a solar furnace. In addition, the two-color pyrometer can be used in conjunction with a conventional brightness pyrometer to determine the effective emissivity of the specimen in the spectral band passed by the brightness pyrometer.

INTRODUCTION

The Hanford Atomic Products Operation has been conducting for the past few years an extensive program of temperature measurement in nuclear reactor systems. Recently, as part of a program of ceramic fuel development, this laboratory has become interested in the accurate measurement of temperatures in a solar furnace and other high temperature devices. This paper presents a summary of the results of a study conducted in order to determine the equipment and techniques currently available for accurately measuring temperatures in the range room temperature to 3500°C.

EQUIPMENT AND TECHNIQUES

The study revealed that many techniques and devices are available or under investigation at the present time for the accurate measurement of temperatures in the extreme range previously mentioned.[1-5] Of those considered, namely, brightness pyrometers, total radiation pyrometers, noise thermometers, thermocouples, and two-color pyrometers, only the latter two were found to be functionally suitable for the accurate measurement of temperatures in a solar furnace.

A. Thermocouples

(1) Advantages

For application in a solar furnace thermocouples have several distinct advantages, namely:

(a) take up little space and can be installed in restricted locations within the unit,
(b) light in weight and construction,
(c) easy to assemble and maintain,
(d) readily subjected to miniturized instrumentation,
(e) the thermal emf is a direct measure of the true temperature (i.e., independent of the emissivity of the material being heated).

(2) Disadvantages

They possess several disadvantages, however, which can offset all the previously mentioned advantages. These are:

(a) chemical reactivity of the thermocouple metals with the environment under measurement,
(b) physical deterioration of the thermocouple due to annealing and recrystallization of the thermocouple wires.

(3) Characteristics

Within the temperature range from room temperature to 1100°C, there are several excellent thermocouples which can be used with various atmospheres. The couples illustrated in Fig. 1 were chosen over others on the basis

FIG. 1.

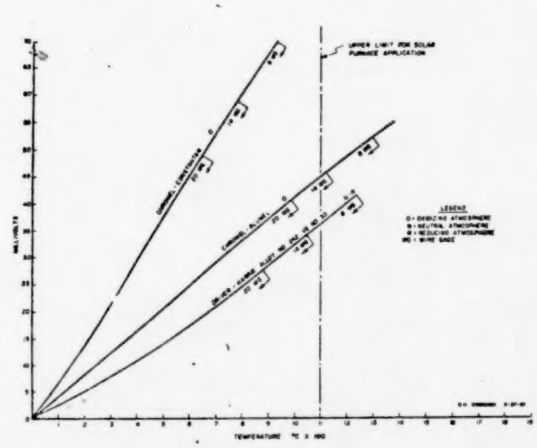

of the following characteristics:

(a) high thermal emf,
(b) linear relationship between temperature and emf,
(c) chemical and physical stability in the environment under measurement and within the temperature range being investigated,
(d) ease of fabrication and calibration,
(e) reproduction emf from batch to batch,
(f) availability,
(g) low initial cost.

Where high sensitivity is required and the atmosphere is oxidizing, the chromel-constantan couple can be used. The limit of error of this thermocouple is ± ¾ per cent, and the sensitivity is about 77 microvolts per °C.[6] Chromel has a nominal composition of 90 w/o nickel and 10 w/o chromium. The nominal composition of constantan is 55 w/o copper and 45 w/o nickel. Appropriate wire sizes are indicated in Fig. 1 for the temperature ranges specified.

Another couple which can be used where the atmosphere is oxidizing is the chromel-alumel couple. The sensitivity of this couple is 42 microvolts per °C with an error limit of ± 2¼°C in the O° to 277°C range and ± ¾ per cent in the range 277°C to 1260°C.[6] Alumel has the nominal composition of 94 w/o nickel, 3 w/o manganese, 2 w/o aluminum, and 1 w/o silicon.

A new Driver-Harris couple,[7] No. 242 vs. No. 33, has approximately the same sensitivity as the chromel-alumel couple in the higher ranges and can be used in reducing as well as neutral atmospheres. The limit of error of this couple is about ± ¾ per cent. The nominal composition of the No. 242 alloy, Geminol P, is 20 w/o chromium, 1 w/o niobium, 1 w/o silicon, and 78 w/o nickel. The No. 33 alloy, Geminol N, is 3 w/o silicon and 97 w/o nickel.

B. Two Color Pyrometers

(1) Emissivity and Reflectivity Problem

The heat fluxes and temperatures in a solar furnace are such that most materials being heated are molten or highly reactive. Radiation pyrometry (optical, color, or total) becomes a necessity, but the application of this technique is beset with problems. Accurate determination of temperatures with radiation pyrometers requires the knowledge of the effective emissivity of the material whose temperature is being measured. Little, if any, data exists on emissivities of materials at temperatures above 2000°C.[1-3,8-20] The presence of oxides, metallic compounds, unknown surface conditions, vapors and atmospheres, and other environmental effects often makes it difficult to know the effective emissivity accurately under existing experimental conditions. The formation of a cavity at the focus of the solar furnace will help in approximating blackbody conditions, but since the focused radiation converges upon the sample through a cone of very large angle no really effective blackbody cavity can be formed. What is needed is a device to read true temperatures independent of emissivity and environmental effects. A device which accomplishes this with a high degree of accuracy is the two-color pyrometer. The operating principles of this device are outlined below. It should be pointed out that measurements using the two-color pyrometer, like those using any radiation pyrometer, must be made under conditions in which only radiation emitted by the body whose temperature is being measured are seen by the pyrometer. Reflected sunlight must be prevented from entering the pyrometer. A solution to the problem of reflected radiation has been described by W. M. Conn and G. Braught.[21]

(2) Principle of Operation

The operation of the two-color pyrometer is based on the principle that as the temperature of a body increases the energy radiated at each wavelength increases. The rate of increase is greater for short wavelengths than for long. Consequently, the ratio of the energy radiated in a selected band of short wavelengths to that radiated in a selected band of long wavelengths increases with temperature, and to each ratio there corresponds a definite temperature, thus

$$\frac{E_s}{E_l} = f(T) \qquad [1]$$

It is possible to express the true temperature, T, (or a close approximation) in terms of this ratio, and if suitable circuitry is provided the temperature may be continuously recorded. The method applies to the measurement of temperature of any material for which the effective emissivities of the two wavelength bands are equal and for which the effective transmissivities of intervening atmospheres and windows in the two wavelength bands are equal. Thus, the method is applicable not only to blackbodies and graybodies but also to materials which conform to the above requirements. Let us examine in detail the principles involved in two-color pyrometry.

The brightness pyrometer provides a measure of the amount of energy radiated by the specimen being viewed in a wavelength band approximately 300 A° wide. The radiant energy received by the pyrometer is given by

$$E = C_1 \int_0^\infty t_\lambda \epsilon_\lambda \lambda^{-5} \exp(-C_2/\lambda T)\, d\lambda \qquad [2]$$

where C_1 and C_2 are known constants, ϵ_λ is the spectral emissivity of the source, t_λ is the spectral transmissivity of the pyrometer, and T is the true temperature. If both the spectral emissivity, ϵ_λ, and the true temperature are unknown, the brightness pyrometer as ordinarily used cannot give a true indication of either the temperature or the emissivity of the specimen. A close approximation to both the emissivity and the true temperature can be determined by using two brightness pyrometers with different t_λ. Ideally the two pyrometers should transmit adjacent narrow wavelength bands so that ϵ_λ can be considered a constant throughout the spectral bands transmitted. If this is the case then the integral of Equation [2] can be reduced to the following:

$$E_s = C_1 t_s \epsilon \lambda_s^{-5} \exp(-C_2/\lambda_s T)\, \Delta\lambda \qquad [3a]$$

and

$$E_l = C_1 t_l \epsilon \lambda_l^{-5} \exp(-C_2/\lambda_l T)\, \Delta\lambda \qquad [3b]$$

for the "short and long" wavelength bands respectively.

Equations [3a] and [3b] may be rewritten, thus

$$\frac{1}{T}=\frac{1}{T_s}+\frac{\lambda_s}{C_2}ln\,\epsilon \qquad [4a]$$

and

$$\frac{1}{T}=\frac{1}{T_l}+\frac{\lambda_l}{C_2}ln\,\epsilon \qquad [4b]$$

where T_s^{-1} and T_l^{-1} represent the expressions

$$\frac{\lambda_s}{C_2}ln\,\frac{C_1\,t_s\,\Delta\,\lambda}{E_s\,\lambda_s^5} \text{ and } \frac{\lambda_l}{C_2}ln\,\frac{C_1\,t_l\,\Delta\,\lambda}{E_l\,\lambda_l^5}$$

In this form T_s and T_l are the temperatures indicated by the brightness pyrometers. These two equations are sufficient to determine the true temperature T and the spectral emissivity of the specimen if suitable values for λ_s and λ_l are independently determined.

In actual practice the pyrometer filters transmit rather broad wavelength bands so that the approximations of Equations [3a] and [3b] are not valid. In the case of incandescent solids the spectral emissivity is relatively constant over limited spectral ranges at a given temperature, and Equation [2] may be written:

$$E_s = C_1\,\epsilon_s \int_0^\infty t_{\lambda s}\,\lambda^{-5}\exp\left(-\,C_2/\lambda\,T\right)\,d\,\lambda \qquad [5a]$$

$$E_l = C_1\,\epsilon_l \int_0^\infty t_{\lambda l}\,\lambda^{-5}\exp\left(-\,C_2/\lambda\,T\right)\,d\,\lambda \qquad [5b]$$

The dependence of t_s and t_l on λ is assumed to be known. The energies of E_s and E_l are related to the brightness temperatures T_s, T_l and the true temperature in the following way,

$$\frac{E_s}{E_l}=\frac{\epsilon_s\,F_s\,(T)}{\epsilon_l\,F_l\,(T)}=\frac{F_s\,(T_s)}{F_l\,(T_l)} \qquad [6]$$

where

$$F_s\,(T)=C_1\int_0^\infty t_{\lambda s}\,\lambda^{-5}\exp\left(-\,C_2/\lambda\,T\right)\,d\,\lambda\text{, etc.} \qquad [7]$$

If it is assumed that $\epsilon_s = \epsilon_l$, the temperature T may be determined as a function of T_s and T_l.

Three types of two-color pyrometers can be recognized. Type I consists of two brightness pyrometers with different spectral transmissivities. In use each pyrometer indicates an apparent temperature. These temperatures are related to the true temperature T in the manner indicated by

$$\frac{\epsilon_s\,F_s\,(T)}{\epsilon_l\,F_l\,(T)}=\frac{F_s\,(T_s)}{F_l\,(T_l)} \qquad [8]$$

or by Equations [4a] and [4b].

Type II gives a response proportional to the ratio of radiant energies in the two-color bands or to the logarithm of this ratio and is characterized by the equation

$$\frac{E_s}{E_l}=\frac{\epsilon_s\,F_s\,(T)}{\epsilon_l\,F_l\,(T)} \qquad [9]$$

Type III employs the principle of equalizing the energies received in both color bands by means of adjustable apertures or color wedges. This type is characterized by the equation

$$\epsilon_s\,F_s\,(T) = t\,\epsilon_l\,F_l\,(T) \qquad [10]$$

where t represents the adjustable transmission coefficient of the aperture or wedge.

In all cases it is necessary to assume that $\epsilon_s = \epsilon_l$.* The successful application of two-color pyrometer techniques depends upon the selection of filters which tend to make the effective emissivities equal. In an article on the theoretical characteristics of bichromatic pyrometers of Type II, Henne[22] concludes that the two pass bands may be close to each other in frequency — in fact they may overlap to a large extent — and the band widths should be large (1000 A - 5000 A). Furthermore, for maximum energy collection the two overlapping wide pass bands should be in the red part of the spectrum.

(3) Pyrometers Already Constructed

Hottel and Broughton[23] used a Type I two-color pyrometer to determine the true temperature of luminous gas flames and reported measurements of temperatures in the 1700°K range with accuracies of ± ¼ per cent or better.

Russel, Lucks, and Turnbull[24] have described a Type II two-color pyrometer. Two models are described. One is portable and the other is a recording type. Both employ photocells in a bridge circuit whose output is proportional to the ratio E_s/E_l. The logarithm of this ratio is proportional to $1/T$. They report accuracies of ± 10°K at temperatures up to 2000°K. Their pyrometer is a d-c instrument, and the authors admit some difficulty with stability.

A beam-splitting Type III two-color pyrometer employing a-c amplification to detect a null point has been described by Gibson.[25] In the temperature range from 273°K to 1473°K a setting and reading accuracy of ± 3°K was reported. This report gives the details and principles of the amplifier design and suggests further improvements.

The German steel industry has used two-color pyrometers to monitor blast furnaces for 15 or 20 years. G. Naeser and W. Pepperhoff[26,27] describe in detail a two-color pyrometer similar to that of Russel, Lucks, and Turnbull[24] except that they have added a computing circuit to get an output directly proportional to the reciprocal of the true temperature. Boos and Willems[28] mention but do not describe a two-color optical pyrometer. They state that numerous comparisons between the immersion pyrometer and the color pyrometer show full agreement (± 10°K) between both instruments. They were measuring temperatures ranging from 1820°K to 2020°K. They also state that many years (15 to 20 years) of measurements with a two-color pyrometer and immersion pyrometers in German steel mills have established that temperature measurements with incandescent disappearing filament pyrometers lead to entirely false conceptions and are useless for the temperature evaluations of a smelting process.

The use of a two-color pyrometer in the French steel industry is discussed by Roduq and Maillot.[29] They also report agreement between two-color pyrometer and

*This is a sufficient condition. Blackbody or graybody conditions need not exist except for the portion of the radiation spectrum to which the color pyrometer is sensitive.

immersion pyrometer temperatures to within ± 10°K and cite the insensitivity of the two-color pyrometer to the introduction of coal dust or water vapor in the light path.

A color temperature comparator has been built by Brown.[30] It is similar in principle to that of Gibson,[25] but, since it employs a diffuser as a receiver of incident radiation, it is said to be relatively insensitive to errors in aiming the instrument at the object to be measured. A reading and setting accuracy of ± 2°K is claimed for the instrument in the 2500 to 3120°K temperature range.

Pyatt[31] has compared the theoretical performance of brightness and two-color pyrometers. His conclusion is that if the emissivity is known reasonably well the brightness pyrometer is often more accurate. He gives charts showing the range of emissivity values for which the brightness pyrometer is more accurate than the two-color pyrometer and visa versa. As previously mentioned, little is known of the emissivities of substances above 2000°C, and it is this very fact which limits the effectiveness of the brightness pyrometer for solar furnace work. Futhermore, it is often difficult to make an educated guess of the emissivity because of oxide films and atmospheres of undetermined transmissivities. The experience of the German steel industry indicates that even when emissivities might be expected to be known, the two-color pyrometer proves to be much superior to the brightness pyrometer. Pyatt[31] also suggests a more complex type of "ratio" pyrometer.

There are several two-color pyrometers commercially available which are designed primarily for use in color photography. One instrument is made in Germany under the trade name Kelvilux and distributed by Mitropia Corporation, New York. Its scale reading accuracy is ± 25°K in the range 2000 to 6000°K and ± 50° in the range 6000°K to 10,000°K. Light intensities between 300 and 100,000 lux are required for accurate readings. An opal-glass receiving surface must be uniformly illuminated with the light from the radiating body whose temperature is being measured. The Kelvilux is an inexpensive instrument costing about $100.

The Rebikoff color temperature meter is similar to the Kelvilux in operation, accuracy, and price. It is made in Switzerland and distributed in this country by Karl Heitz, New York.

Development work is being done at HAPO[32] on a two-color infrared pyrometer similar in design to that described by Gibson.[23] While this instrument is intended for use on a hot stage of a metallograph, it is hoped that slight modification will make possible its use in solar furnace temperature measurements.[33] In this case, it is intended that the two-color pyrometer will be sensitive enough to operate through the eyepiece of a Baumann-type high temperature microscope.[34] The pyrometer will be synchronized with a rotating cylinder near the focus of the solar furnace so that it reads temperature only when the sample is shaded from the incident sunlight. The microscope, on the other hand, will be used when the sample is brightly illuminated by the incident focused sunlight.

CONCLUSIONS

Instruments and techniques have been developed for measuring accurately the temperature of a specimen being heated in a solar furnace. By choosing the proper thermocouple, specimen temperatures can be measured in the range room temperature to 1100°C with an over-all accuracy of better than ± ¾ per cent. In the range 1100°C to 3500°C; a two-color optical pyrometer will measure temperatures with an accuracy of ± 10°C. In a properly designed system both methods are independent of emissivity and of environmental conditions existing in a solar furnace. The two-color pyrometer can be used in conjunction with a conventional single-color pyrometer to determine emissivities of materials at elevated temperatures.

ACKNOWLEDGEMENT

The authors wish to thank the U.S. Atomic Energy Commission for permission to publish this paper.

DEFINITIONS

Blackbody — A body which absorbs all the radiation incident on it, reflecting none.

Emissivity — The ratio of the radiant energy emitted by a body to the radiation emitted by a blackbody at the same temperature and under similar conditions.

Graybody — A body which has the same emissivity for every wavelength but whose emissivity is less than unity.

Brightness pyrometer — A device which indicates temperature by measuring the energy emitted by a body in a narrow spectral band.

Optical pyrometer — A type of brightness pyrometer in which the brightness of a body is compared to the brightness of a calibrated tungsten lamp. The lamp voltage is varied until the lamp filament has the same brightness as the body as determined by viewing both objects through an essentially monochromatic filter.

Two-color pyrometer — A device which measures temperature by comparing the amounts of energy radiated by the specimen in two different spectral bands.

Total radiation pyrometer — A device which measures temperature by measuring the energy of all wavelengths emitted by the specimen.

NOMENCLATURE

E . . . total radiant energy flux transmitted through a pyrometer

$f(T)$ . . . function of true temperature

C_1 . . . 3.7413 (10^{-12}) watts-sq cm

C_2 . . . 1.4388 cm-degree

ϵ . . . effective emissivity in the wavelength band

t . . . transmissivity

λ . . . wavelength (microns), as a subscript it indicates spectral dependence

s . . . indicates band of shorter wavelengths

l . . . indicates band of longer wavelengths

e . . . logarithmic base

T . . . temperature °K, subscripts l, s, and B indicate brightness temperatures in limited spectral ranges

$$F(T) \ . \ . \ . \ C_1 \int_0^\infty t_\lambda \lambda^{-5} \exp\left(-C_2/\lambda T\right) d\lambda$$

REFERENCES

1. *High temperature — a tool for the future.* Menlo Park, Calif., Stanford Research Institute, 1956. p. 190-94.
2. *Temperature, its measurement and control in science and*

industry, Vols. I and II. N.Y., American Institute of Physics, Rheinbold Pub. Corp., 1941 and 1955.
3. *High temperature technology;* ed. by I. E. Campbell. N.Y., J. Wiley, 1956.
4. H. W. Maynor, "Primary investigation of literature dealing with the measurement of excessively high temperatures." NEPA-745, Aug. 27, 1948. 12 p.
5. P. H. Dike, "Thermoelectric thermometry." Leeds and Northrup Company. p. 13.
6. "Reference tables for thermocouples." *Nat. Bur. Standards, Circular* 561, Apr. 27, 1955.
7. C. L. Guttel, "A new thermocouple for service in reducing atmospheres." *Am. Soc. Testing Materials, Bull.* No. 216: 64-65, Sept. 1956.
8. M. P. Bauleke, "Spectral and total emissivity: a guide to the literature (1910-1951)." ISC-364, June 1, 1953, 41 p.
9. J. G. Darward and D. Aeed, "Heat radiation and emissivity measurements." Univ. of California, Berkeley, Radiation Lab., RL-8. 6. 5., May 6, 1944.
10. F. H. Norton, *Refractories.* N.Y., McGraw Hill, 1949. p. 502.
11. *Ceramics, a symposium;* ed. by A. T. Green and G. H. Stewart. Stohl-on-Trent, British Ceramic Society, 1953. p. 695, 722-23.
12. F. H. Norton, W. D. Kingery, A. L. Loeb, J. Frovel, R. L. Cable, and T. Vasilos, "Measurement of thermal conductivity of refractory materials." NYO-3647, 1953.
13. A. H. Sully *et al*, "Some measurements of the total emissivity of metals and pure refractory oxides and the variation of emissivity with temperature." *Brit. J. App. Phys.* 3:97-101, 1952. (Includes cerium, thorium, magnesium oxides.)
14. R. Uzan, "Some results of spectral and thermionic emissivity measurements on ceric oxide." *Le Vide* 7:1139-40, 1952. CA 46:5904h.
15. M. Michaud, "Thermal emissivity of metallic oxides and refractories at high temperatures." 4th Congrès Intern. Chauffage Ind., Paris, 1952, Preprint No. 159. 11 p. (Thermal emissivities for SiO_2-Al_2O_3, SiC, and ThO_2, from 1000° to 1600°.)
16. W. Eitel, "Thermal emissivity of refractories and its importance for glass furnace operation." *Glass Ind.* 36:193-97, 228, 1955.
17. M. Michaud, "Thermal emissivity of refractory materials at high temperatures." *Silicates Ind.* 19:243-50, 1954. (Method to determine emission coefficient: monchromatic emission, total emission. True temperature of radiating surface. Al_2O_3, SiO_2, Fe_2O_3.)
18. G. Mesnard, "Thermionic emission and optimum emissivity of zirconium oxide." *Le Vide* 8:1392-99, 1953. CA 48: 3784d.
19. Battelle Memorial Institute, Titanium Metallurgical Lab., "The emissivity of titanium." Columbus, Ohio., Mar. 15, 1957. NP-6255. 7 p. (Data on emissivities of different grades of Ti at various temperatures are summarized.)
20. Illinois Institute of Technology, Armour Research Foundation, "Determination of emissivity and reflectivity data on aircraft structural materials. Part I, Techniques for measurement of total normal emissivity and reflectivity with some data on copper and nickel." WADC-TR-56-222 (Pt.1), June 1956. 50 p.
21. W. M. Conn, "Separation of incident and emitted radiation in a solar furnace by means of rotating sectors." *J.O.S.A.* 44: 45-47, Jan. 1954.
22. H. Henne, "The theoretical characteristics of bichromatic pyrometers." *Brit. J. App. Phys.* 4:374-77, Dec. 1953.
23. H. C. Hottel and E. P. Broughton, "Determination of true temperature and total radiation from luminous gas flames" *Ind. Eng. Chem.* 4(2): 166-74, Apr. 15, 1932.
24. H. W. Russel; C. F. Lucks, and L. G. Turnbull, "A new two-color optical pyrometer." *J. Opt. Soc. Am.* 30:248-50, June 1940.
25. A. F. Gibson, "A two-color infra-red radiation pyrometer." *J. Sci. Inst.* 28:153-55, May 1951.
26. G. Naeser and W. Pepperhoff, "Verfahren zur Ermittlung der Schmelyen-temperature in Blasenden Konverter." *Stahl und Eisen* 70(1): 22-24, Jan. 1950.
27. —— ——"Optical temperature measurements on luminous flames." *Arch. Eisenhüttenw.* 22:9-14, Jan. & Feb. 1951.
28. G. Boos and J. Willems, "Temperaturmessurgen im Seemens Martin Stahlwerk." *Stahl und Eisen* 75(14); 900-906, July, 1955.
29. P. Roduq and G. Maillot, "Le pyromètre à deux couleurs." *Rev. Mét.* 52:477-84, 1955.
30. W. J. Brown, "A physical colour temperature comparator." *J. Sci. Inst.* 31:469-71, July 1954.
31. E. C. Pyatt, "Some consideration of the errors of brightness and two-color types of spectral radiation pyrometers." *Brit. J. App. Phys.* 5:264-68, July 1954.
32. T. K. Bierlein, private communication.
33. H. W. Newkirk and M. K. Millhollen, "Feasibility of a solar furnace for ex-reactor thermal studies." HW-51381, July 1957. unclassified.
34. H. N. Baumann, Jr., "Microscopy of high temperature phenomena.' *Bull. Am. Ceram. Soc.* 27(7): 267-71, 1948.

A GUIDING SYSTEM FOR SOLAR FURNACES

By TIBOR S. LASZLO,* WILLIAM F. de DUFOUR,** and JOSEPH ERDELL***

High Temperature Laboratory, Fordham University, New York City

An electronic system has been developed to guide solar furnaces and instruments of similar axial arrangement in their motion. The driving motors are supplied with a basic current. To this is added algebraically a correction current developed by a photosensing and amplifier system. This arrangement permits precise, even following of the sun's apparent motion. The system is exceptionally free of "hunting."

A 60-in. diameter solar furnace was constructed from an army searchlight in the High Temperature Laboratory of Fordham University for the investigation of matter above 2000°C. Solar furnaces of similar construction have been described by Conn[1] and by Trombe.[2]

The mirror of this searchlight is mounted altazimuthally, and it may be adjusted to any position above the horizontal by rotating it around its horizontal and/or vertical axis. When the solar furnace is used for high temperature research, it is essential that the position of the hot zone on the sample be very stable. This can be achieved by keeping the mirror focused on the sun. Manual focusing results in jerky motion and is therefore unsatisfactory. Mechanical rotation has to be guided so as to follow precisely the apparent motion of the sun.

A guiding mechanism was developed by Straubel[3] for keeping the arc of an electric light in a fixed position. He uses resistance elements with very large temperature coefficients. When the arc moves out of the focus, radiation falls upon the resistance element. The change in resistance starts an electric motor which moves the carbon electrode back into focus. On our furnace this system cannot be used since it has a considerable time lag and low sensitivity.

A method more nearly satisfying our requirements was developed by the Army Medical Corps. They use the selsyn system originally built into the army searchlight. A sun-sensing element consisting of four photocells is mounted on the mirror. When the mirror moves out of focus, the system generates an a-c signal which, through the selsyns, makes two motors turn the mirror back into focus. This system differentiates between elevational and azimuthal movement, has a fast response, and permits rotation in two directions around both axes. The authors point out that this arrangement would cause the searchlight to "home" on the brightest point on the sky. If the sun is momentarily covered by a cloud, the searchlight may move as much as 90° off the sun, only to swing back again when the sun becomes uncovered. It is indicated that this effect may be reduced by decreasing the sensitivity of the system. We also think that the high starting torque and angular momentum of the ¼-hp driving motors may interfere with the accurate motion of the searchlight.

To satisfy our strict requirements in the automatic guiding of a solar furnace, a new system was developed in the High Temperature Laboratory of Fordham University. It is, in principle, a rate servo system. The mirror-drive motors are supplied with a basic current that gives the approximate tracking speed. When the mirror deviates from the correct tracking path, a photosensitive system generates an error signal. This signal, after proper amplification, is algebraically added to the basic drive current thus correcting any inaccuracies in the basic tracking speed.

The original ¼-hp 1725 rpm searchlight-drive motors were replaced by 1/20-hp 4000-rpm 110-VDC shunt gear motors in order to reduce starting torque and angular momentum.

The gear system of the searchlight was so altered that these motors would move the mirror with the basic tracking speed when supplied approximately ¼ of their rated current intensity. This circumstance permits satisfactory speedup when the mirror is lagging behind. At the same time the basic current is in proper proportion to the error signal for correction by the latter.

A photosensitive light receptor was constructed, consisting of four gas phototubes mounted in quadrature at the end of a collimating tube (Fig. 1). The phototubes are optically isolated in individual chambers, and those in opposite quadrants are paired. One pair is aligned parallel to the horizontal axis of rotation of the mirror. The other pair automatically becomes parallel to the vertical axis. The collimating tube is capped by an aperture plate with a round hole centered over the four phototubes. The diameter of this opening is selected to give a spot size just fitting inside one chamber. A diffusion disc is placed in front of the phototube mounting assembly to minimize the effect of variations in cathode surface sensitivity. A filter is mounted in front of the aperture to control the intensity of light reaching the phototubes. The entire

*Present address: Curtiss Wright Corp., Wood-Ridge, N.J.
**Present address: General Electric Co., Schenectady, N.Y.
***Present address: Brooklyn, N.Y.

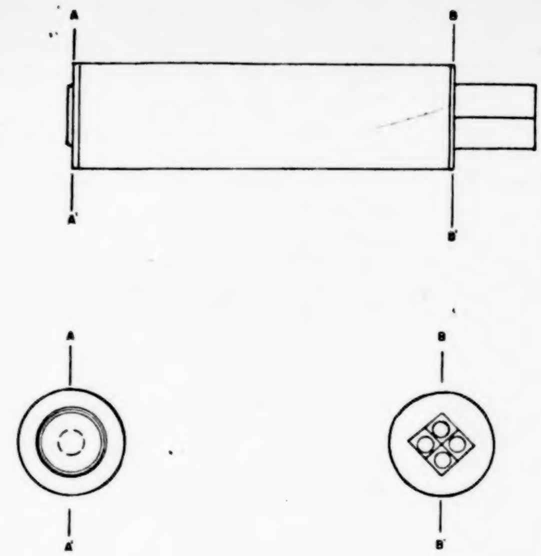

FIG. 1 — Sensing-device phototube assembly.

sensing assembly is mounted on the mirror-housing with the axis of the collimating tube parallel to the rotational axis of the paraboloidal mirror. When the mirror is focused on the sun, an image of the aperture falls on the center of the diffusing disc in such a way as to provide equal illumination to all four phototubes, and hence equal voltage outputs from the tubes. Any deviation from the focus moves the spot off center. This causes unequal amounts of light to fall on the phototubes and results in unequal voltage outputs. The voltage outputs of the phototubes contain the vector magnitude information

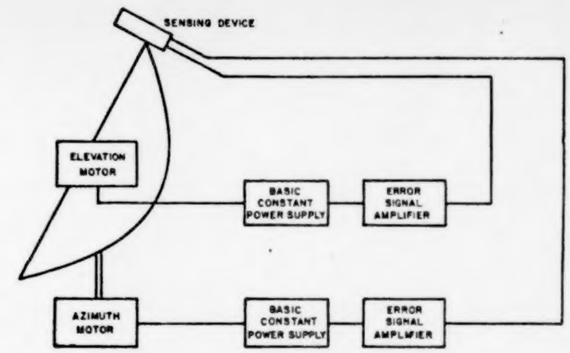

FIG. 2 — Block diagram of driving and guiding system.

which can be used to determine both the direction and magnitude of the spot shift. This information is used in an error-signal amplifier to generate a voltage varying both in polarity and amplitude. The amplified error-signal voltage is added algebraically to the control voltage which determines the basic drive current. The addition of the error-signal voltage corrects any inaccuracies in the tracking speed. If the phase of the error signal is selected so as to provide a faster drive when the sensing head is lagging behind and a slower drive when it is leading, then the system becomes self-balancing. This results in correct tracking. A block diagram of the entire driving and guiding system is given in Fig. 2.

The electronic system for the azimuthal guiding is illustrated in Fig. 3. Two phototubes V_1 and V_2 are mounted parallel to the horizontal axis of the mirror. Equal amounts of light falling on V_1 and V_2 produce equal

FIG. 3 — Circuit diagram of azimuthal guiding system.

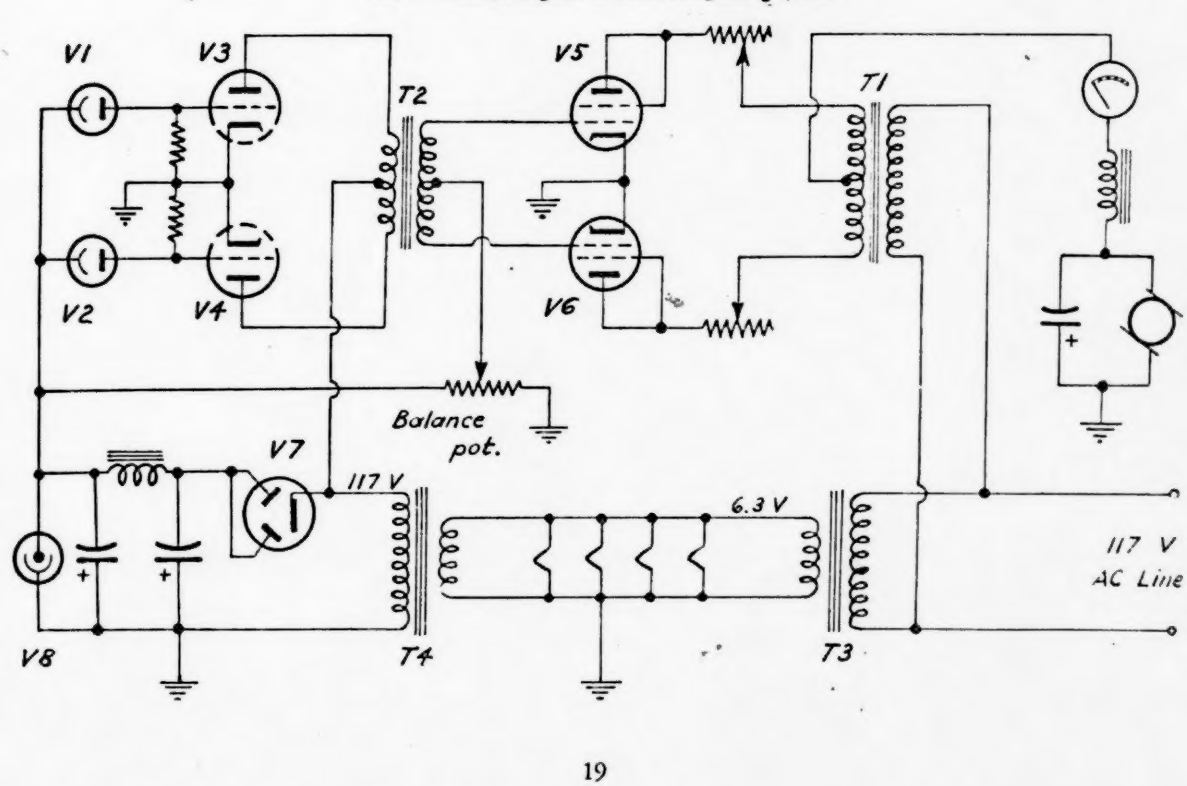

grid voltages on the tubes V_3 and V_4. When the primary side of the transformer T_2 goes positive, V_3 and V_4 conduct according to their grid voltages, and therefore equal plate voltages will be obtained. The voltages across the two halves of the primary coil of the transformer T_2 are opposed to each other, and, since in this case they are numerically equal, the result is zero voltage on the secondary coil of T_2. If, however, unequal amounts of light fall on V_1 and V_2, the voltages across the two halves of the primary coil of T_2 are no longer equal. They are proportional to the amount of grid bias developed by V_1 and V_2. A secondary voltage is then produced on T_2 which is proportional in amplitude to the difference between the plate voltages of V_3 and V_4. The polarity of this secondary voltage shifts depending on which of the two phototubes receives more light.

The basic drive current is supplied to the armature of the drive-motor from a full wave rectifier circuit using two beam power amplifier tubes, V_5 and V_6. Grid bias is obtained for these tubes from the balance potentiometer which is adjusted to give a maximum voltage slightly beyond the cut-off value for V_5 and V_6. The secondary voltage from T_2, i.e., the error signal, is superimposed on the grid bias of V_5 and V_6, thus increasing or decreasing the current to the armature of the drive-motor. Balancing controls for the error signal amplifier tubes are not necessary. Any error signal that will be produced due to the different sensitivity of the phototubes is constant and can be compensated for by the proper setting of the rate potentiometer. On the other hand, the rate at which the system corrects itself may be affected by any unbalance in these tubes. Proper operation, however, has been achieved with phototubes mismatched by as much as 50 per cent.

The electronic system for the elevation guiding is basically the same. Some modification is necessary, however, caused by differences in the nature of rotation. Azimuth tracking is always in the same direction and at the same speed. Elevation tracking requires reversal of direction at the zenith position of the sun and continuous change in angular velocity. The reversal of direction is accomplished by the installation of two relays into the elevation-signal amplifier. The first relay reverses the direction of current from the elevation-control phototube pair. The second relay reverses the polarity of the motor-armature current. The switch of both relays is actuated by an arm mounted on the vertical shaft of the mirror. When the mirror reaches the 12 o'clock noon position, the arm throws the switch which in turn energizes the relays, thus reversing the elevational rotation of the mirror. The rotation of the vertical shaft is used also for the change in angular velocity of the elevational rotation. A center tapped rate potentiometer is mounted in the stationary base of the searchlight. The rotation of the vertical shaft is transmitted by gears to the moving contact of the potentiometer. As the vertical shaft rotates towards the 12 o'clock noon position, the rate potentiometer decreases the basic drive current of the elevation motor. At 12 o'clock noon (astronomical time) the angular velocity of the motor is zero. Accordingly the output of the rate potentiometer is also zero. After 12 o'clock the basic drive current increases, and, since the polarity of the armature current was changed by activation of the relay, the mirror rotates towards the horizon. Superimposed on this changing basic drive current is the amplified error signal correcting any deviations from the true tracking speed as described in connection with the azimuthal system.

The constant field current to both motors is supplied by a selenium full-wave rectifier.

In operation, this system shows the following advantages: high sensitivity and complete absence of "hunting," that is, overcorrection. In addition it was found that the passing of a cloud in front of the sun does not upset the tracking. Since in this case no error signal is furnished by the phototubes, the driving motors receive only the basic drive current. Accordingly, the mirror will follow approximately the apparent rotation of the sun in spite of the screening effect of the cloud. When the cloud passes, the mirror may be somewhat off the true position due to the absence of correction. This deviation, however, will be immediately corrected when the phototubes receive direct sunlight and the precise tracking is resumed.

ACKNOWLEDGEMENT

The authors wish to express their appreciation to the National Science Foundation for a grant supporting their work.

REFERENCES

1. W. Conn, "Gesichtspunkte für den Entwurf von Sonnen-Spiegelofen für Hochtemperaturforschung und -Entwicklung." *Z. Angew. Phys.* 6:284-91, 1954.
2. F. Trombe, "Le Laboratoire de l'Energie Solaire de Mont-Louis." *Bull. Soc. Chim. France* 4:353-68, 1953.
3. H. Straubel, "Kontinuierlich arbeitende Brennpunkteinstellung für Bogenlampen." *Z. Tech. Phys.* 22:283-87, 1941.

A PRESENTATION OF SOLAR RADIATION DATA OBTAINED BY A SPECTROHELIOMETER

By Y. T. SIHVONEN, R. F. MAJKOWSKI, and W. SLATER

Research Staff, General Motors Corporation, Detroit, Michigan

An instrument that measures solar radiation has been fabricated and put into operation. This instrument, called a spectroheliometer, continuously records and integrates the sun's radiant power in five selected wavelength intervals, and in addition incorporates a pyrheliometer to measure over-all solar radiation. The individual spectral bands covered are 3095-3260 A, 3410-3630 A, 3865-4150 A, 4420-4900 A, and 5385-6295 A. Spectroheliometer data taken in tests near Miami, Florida, from February 1954 to August 1956 give information concerning the approximate solar power and energy distribution curves and the effects of season, time of the day, meterological conditions, etc., upon them. During a full year of Florida operation the energies received in the individual spectral bands (in order of increasing wavelengths) were 0.195, 1.28, 2.83, 8.41, and 20.37 watt-hours per sq cm. The direct solar-noon power distribution curve obtained in Florida shows good correlation with other published data, but indicates a slightly higher distribution at the longer wavelengths and a need to increase the accepted value of the solar constant from 1.94 cal per min per sq cm.

A comparison made between Detroit, Michigan and Miami, Florida sunshine reveals an interesting phenomenon called "solar twinkle," an irregular repetitive variation in solar radiation reaching the ground which is thought to be due to excessive foreign particles in the atmosphere and or some form of atmospheric turbulence.

INTRODUCTION

Many individuals and groups, including these laboratories, are interested in solar radiation and its magnitude upon exposed panels used in outdoor weathering and solar energy studies. This interest has led to the design and fabrication of an instrument called a spectroheliometer,[1] which is capable of continuously measuring the amount and approximate spectral distribution of solar radiation and transposing this information to a plane of any desired orientation. The spectroheliometer was first tested in Detroit, Michigan and was then put into operation near Miami, Florida, where it continuously monitored solar radiation until August 1956.

Basically the spectroheliometer is a quartz spectrograph which employs five thermopiles placed at the focal plane to measure the intensity of solar radiation, i.e., solar power per unit area, in five selected wavelength intervals. Collectively, these five spectral bands span a range from the near ultraviolet to the upper limits of the visible. Individually, these bands encompass wavelength intervals from

3095 A — 3260 A . . . channel 1
3410 A — 3630 A . . . channel 3
3865 A — 4150 A . . . channel 5
4420 A — 4900 A . . . channel 2
5385 A — 6295 A . . . channel 4

The channel designations given are those assigned these spectral bands in the spectroheliometer's amplifying and recording units. The spectroheliometer also incorporates a 50-junction Eppley Pyrheliometer (channel 6) to measure gross radiation.

Since its optical portions continuously face the sun, the spectroheliometer initially samples direct solar radiation and then automatically converts these direct radiation measurements into panel radiation measurements. The process of converting direct radiation measurements into panel radiation is referred to in this paper as compensa-

FIG. 1 — A typical daily record (near Miami, Feb. 10, 1954) indicating radiation received by a panel facing south and inclined 45°. Each channel's output must be multiplied by a calibration factor before absolute radiation intensity is known.

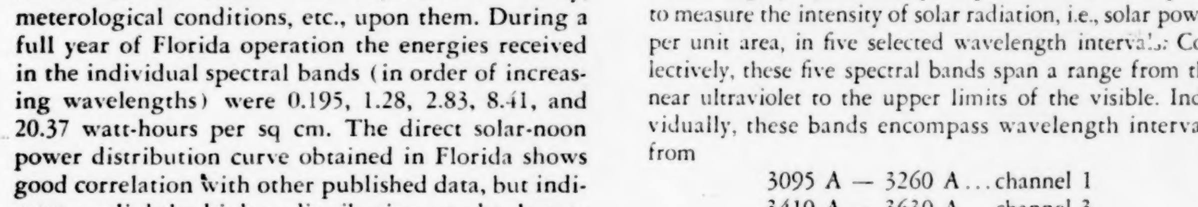

tion. Either direct or compensated signals are then recorded by a multipoint print recorder on a strip chart as shown in Fig. 1. From this chart it is possible to compute instantaneous solar power in each of the six channels as a function of time of day, and hence the approximate spectral solar power distribution at any selected time of the day.

The radiant power signals in each channel are also integrated by means of special watt-hour meters. From the readings of these integrators, the amount and approximate spectral distribution of solar energy (solar energy equals integrated solar power) are obtained.

Compensation is most easily understood by considering solar radiation as a vector. Direct solar radiation can be defined as that radiation falling on a surface whose normal is continuously directed towards the sun. The direct solar radiation vector is directed along this normal, and the amount of direct radiation is the magnitude of this vector. Panel radiation, i.e., the radiation falling on a stationary panel of any desired orientation, can be considered as the component of the direct radiation vector along the normal of the panel in question. Thus, direct radiation can be converted to panel radiation by computing its projection along the normal to the stationary panel.

Compensation is accomplished by multiplying the magnitude of the direct radiation vector by a double cosine function $\cos \alpha \cos \beta$. α is defined as the angle between the panel normal and the incident radiation vector, measured perpendicularly from the north-south plane passing through the normal. Its rate of change equals 15° an hour. The mode of change of $\cos \alpha$ during the day is shown in Fig. 2. β is the angle between the panel normal and incident radiation vector measured in the north-south plane passing through the normal and is a function of latitude inclination of the panel and solar declination. The seasonal variation of $\cos \beta$ for a panel inclined 45° facing south during the period from February 1954 to August 1955 is shown in Fig. 3. In practice, β can be considered to be constant for any given day but varies slightly from day to day, while α varies continuously throughout the day, following the curve shown in Fig. 2 and measured relative to solar noon. In brief, multiplication by $\cos \alpha$ gives the component of direct radiation in the plane of the prime meridian, and $\cos \beta$ projects this component onto the panel normal.

The compensating circuitry[1] which is employed in the spectroheliometer can be simply altered to take care of

FIG. 2 — The mode of change of cos α throughout the day. Plus hours are after solar noon; minus hours are before.

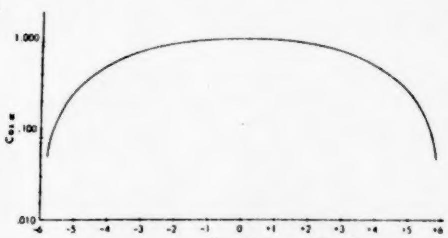

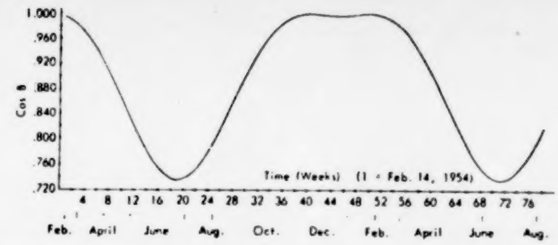

FIG. 3 — The mode of change of cos β relative to a 45° panel facing south for an 18-month period from February 14, 1954 to August 14, 1955 at lat. 25° 47′ N, long. 80° 16′ W (near Miami).

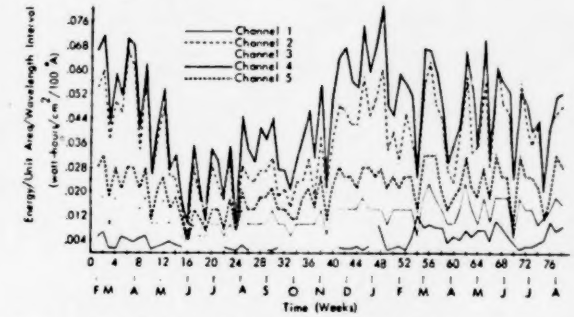

FIG. 4 — Weekly integrated compensated radiation per unit wave length interval during a 1½-year period (near Miami).

panels oriented in any direction* or may be bypassed, so that direct solar radiation is recorded.

INTEGRATED SOLAR RADIATION DATA

Of the two types of spectroheliometer data available, the first to be discussed will be integrated solar radiation data. This type of information is obtained from the readings of the watt-hour meters associated with each channel. The unit integrating period used during the Florida tests was one week. Fig. 4 shows the total weekly radiant energy per unit wavelength interval for panel radiation in the five spectral channels as a function of 78 one-week periods extending from February 14, 1954 to August 14, 1955. The curves start at a relatively high value in February-March, drop during April-May to a low in June-July, rise again in August-September-October to a peak during November-December-January, and start to decline again in February. The general decline of radiant energy in the spring and summer months and its peaking during the months of late fall and early winter follows the attenuation depicted in Fig. 3 by which direct radiation is transformed into panel radiation. The abrupt variations can be attributed to sporadic weather conditions from one week to the next. It will be noted that the curve for channel 1 is not continuous. This resulted from occasional interruptions in the normal operation of this channel. The crossing of channel 1 and 3 on the 54th week is due to a malfunctioning of channel 1, while the occasional crossings of channels 2 and 4 are attributed to weather condi-

*This would involve knowing the angle of incidence of solar radiation on a desired panel, in order to determine its projection on the panel normal. For this information see F. Benford, "Duration and intensity of sunshine. Part I, General equations and corrections." *Illum. Eng.* 42: 527-44, May, 1947.

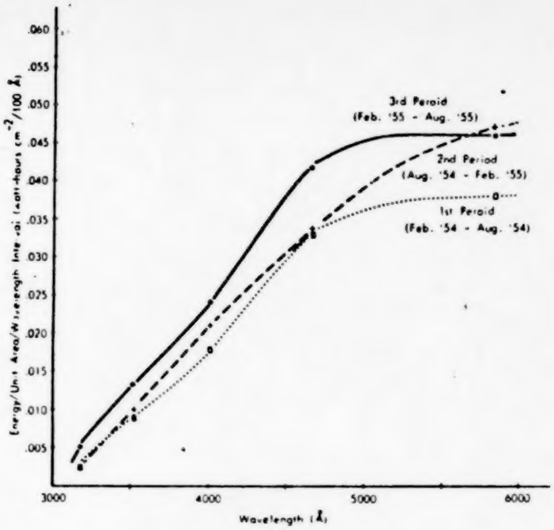

FIG. 5 — Energy distribution curves for panel radiation for the three consecutive 26-week segments in the interval from February 14, 1954 to August 14, 1955.

tions and/or reading errors. Corrections for down time were made on the basis of preceding and following week's results, and from the recorded weather conditions.

The radiant energy having fallen in each channel over a longer unit period may be measured from the type of data shown in Fig. 4 by integrating the area under the curves, or taken directly from the spectroheliometer integrators. Thus, it was determined that in one year (February 1954 to February 1955), at lat. 25° 47′ N, long. 80° 16′ W (near Miami), the following solar energy was received by a test panel facing south and inclined 45°:

Band (angstroms)	Energy received (watt-hours/cm²)
3095-3260	0.195
3410-3630	1.28
3865-4150	2.83
4420-4900	8.41
5385-6295	20.37
Pyrheliometer	119.83

Using data of the type shown in Fig. 4, different studies have been made concerning environmental influences upon the spectral distribution of solar energy, such as: effects of average weekly weather conditions, effects of various months or seasons, effects of air mass, etc. As an example of these studies consider the total energy distribution curves, shown in Fig. 5, which are plotted for the three consecutive 26-week periods that compose the total 78-week interval of Fig. 4. Each curve represents the accumulated energy over the 26-week period. In each of these energy distribution curves, the value of radiant energy per unit wavelength interval for each individual channel of Fig. 4 has been plotted against the mid-wavelength of the corresponding spectral band. Because of the relatively broad width of the spectral band associated with each channel, the energy distribution curves thus obtained average out minor fluctuations.

It can be seen in Fig. 5 that the energy distribution curves for the first and third 26-week periods (like periods of the year; February-August) have very similar slopes, with the third-period curve having greater magnitude because of more favorable weather conditions. The distribution curve for the second 26-week period (August-February) is quite different from that of the other two periods, and it can be concluded that proportionately less 5000 A-6000 A radiation is available during the first half of a year than in the second half. This is a reasonable result if air-mass differences and the selective effects of these masses on the radiation are considered.

INSTANTANEOUS SOLAR POWER

The integrated radiation data treated above are affected by a large variety of weather conditions that can be present during the integrating period. These introduce serious limitations in the use of this type of data for certain studies. However, with respect to weather conditions, instantaneous solar power data (Fig. 1) are limited only by the particular weather present at the moment measurements are made, and it is possible to select a uniform set of conditions (i.e., type of weather and time of day) under which a study is to be made. The power value is calculated by multiplying the scale displacement by a predetermined (calibrated) radiant power scale factor (radiant power/scale division). Test signals in each channel are put on each daily chart to help determine these scale factors, which are different for each channel.

As an example of a study using this type of information, consider Fig. 6, which shows the spectral distribution of radiant power for panel radiation at solar noon for the same three consecutive 26-week periods used in Fig. 5. For these curves, 18 clear days were chosen, approximately four weeks apart. Each distribution curve in Fig. 6 represents the average solar noon radiant power on six of these days. It can be seen that the instantaneous solar noon power distribution curves for all three periods are similar in slope, whereas the solar energy distribution curves,

FIG. 6 — Average solar noon power distribution curves for the same three 26-week intervals as in Fig. 5.

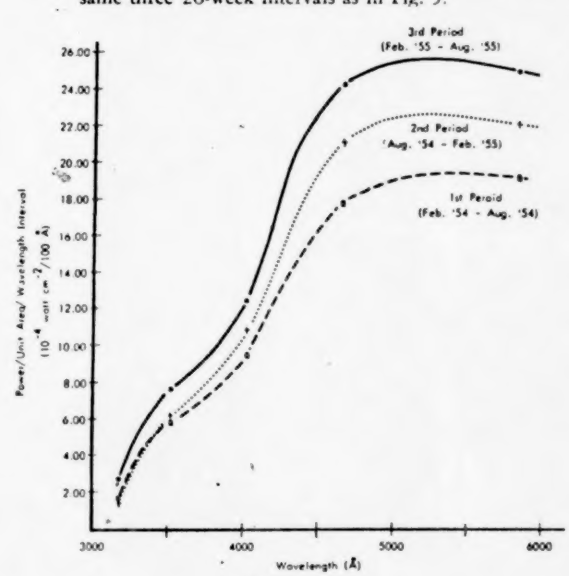

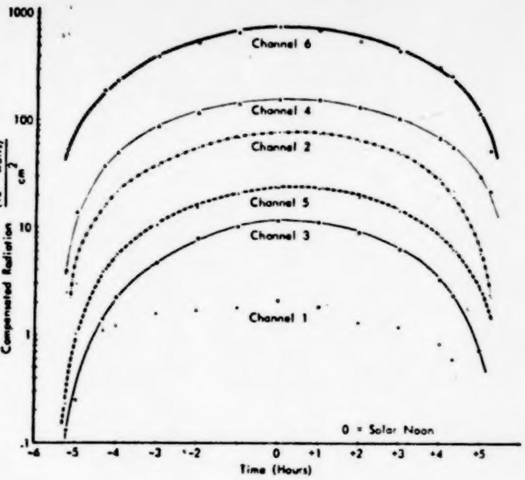

FIG. 7 — Solar power chart for panel radiation for May 8, 1954. This chart illustrates the solar radiation in each of the six spectroheliometer wavelength intervals as a function of time of day.

Fig. 5, show quite a variation in the second 26-week period. With respect to relative magnitudes, the positions of corresponding curves of Figs. 5 and 6 are unchanged.

As mentioned previously, a graph may be made from the spectroheliometer record charts, in which is plotted the instantaneous solar power in each of the six channels as a function of time of day. Such a graph, illustrating panel radiation and called a daily solar chart, is shown in Fig. 7. A logarithmic ordinate is used so as to accommodate all six channels. Time is measured relative to solar noon with zero on the abscissa defined as solar noon, and minus hours meaning before and plus hours after solar noon. Daily solar power charts have also been constructed illustrating direct radiation. The radiant power curves for direct radiation show much less curvature through the day than the corresponding curves of the panel radiation charts, but show a sharper increase and decrease in solar radiation at sunrise and sunset.

FIG. 8 — Solar power distribution curves for panel radiation at various hours on May 8, 1954. This graph illustrates the hourly variation in the radiant power distribution. Zero hour is defined as solar noon. Plus hours are after, minus hours are before solar noon.

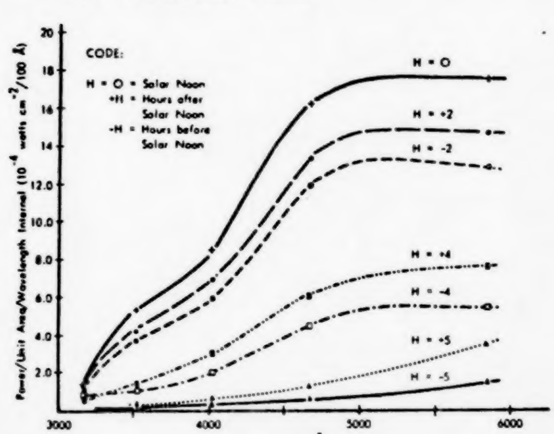

From daily solar power charts such as Fig. 7, the hourly variation in radiant power distribution has been studied. Fig. 8, which was obtained from the data of Fig. 7, illustrates the change in the spectral distribution of radiant power at various hours of the day. It is interesting to note that solar radiation is not maximum at solar noon. In Miami this has been found to be generally the case, with maximum radiation occurring sometimes as much as 30 minutes after solar noon. One explanation for this is the asymmetrical effect of humidity, which is usually high in the morning, and relatively low by mid-afternoon.

COMPARISON OF SPECTROHELIOMETER RESULTS

The spectroheliometer is a different means of gaining solar radiation information; hence, it is of interest to compare results with data obtained by other methods. The spectroheliometer data chosen for this comparison is the solar noon radiation distribution curve. This type of curve was selected because of the availability of similar, well accepted curves in the literature, and second because of its freedom from gross weather effects.

Two comparison curves were selected and are plotted in Fig. 9. The first is a compilation by Parry Moon[2] of the results of many experiments performed by different investigators from 1903 to 1932. The second comparison curve is the result of four days' observation during July 1953 in New Mexico by National Bureau of Standards.[3] Both comparison curves are given in terms of direct radiation, while the spectroheliometer curve is given in terms of panel radiation which, over the 19-month period of investigation, amounts to approximately 90 per cent of direct radiation. The two comparison curves are given in terms of a theoretical air-mass thickness of one. This thickness refers to the secant of the zenith angle of the

FIG. 9 — Comparison between the average spectroheliometer solar power distribution curve and two other accepted solar radiation distribution curves.

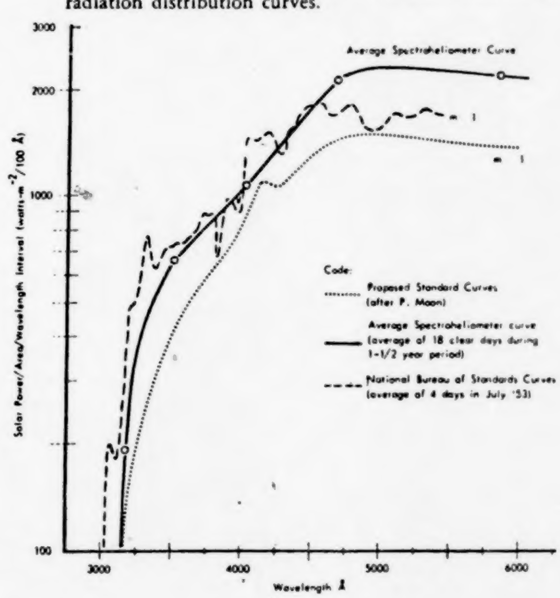

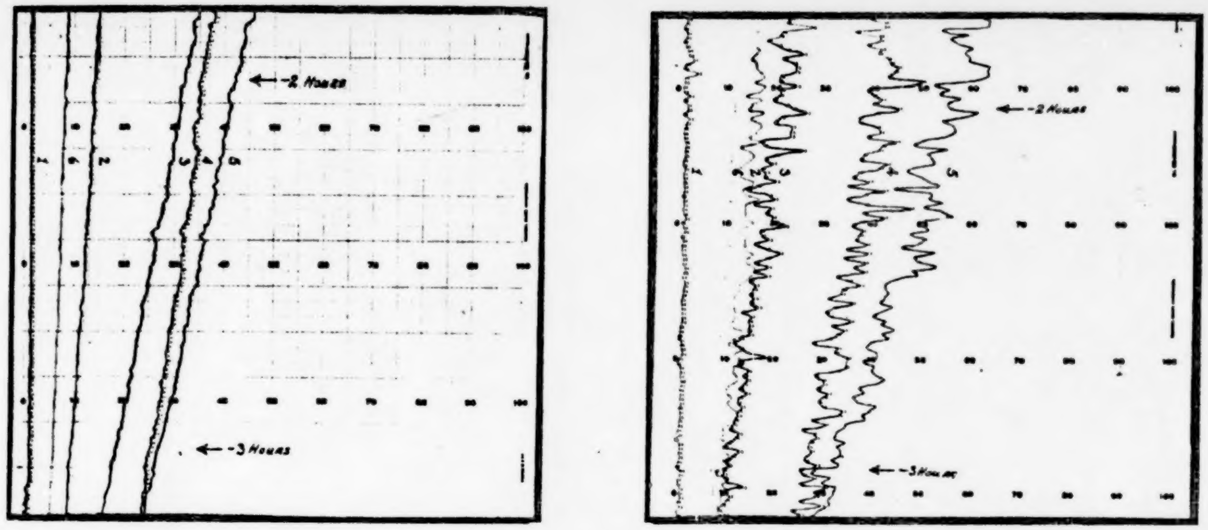

FIG. 10 — It is felt that industrial atmospheres give rise to random variations in solar intensity. Above is a record made in Detroit on October 16, 1953 over the period of 3 to 2 hours before solar noon. Below is a record made near Miami on October 20, 1954 over the same interval. Each record was taken on a "clear" day.

sun and has nothing to do with the physical make-up of the air mass. The theoretical air-mass thickness for the spectroheliometer curve is 1.17.

The shape of the spectroheliometer distribution curve follows closely that of the proposed standard irradiation curve of Moon. Because of the relatively large width of the spectroheliometer wavelength bands, the slight "hump" noted in the Moon curve between 4000 A and 4100 A is not apparent. With respect to magnitude, the spectroheliometer curve follows closely that of the N.B.S. curve up to 4600 A. Both the N.B.S. and the spectroheliometer curves are higher in magnitude than Moon's irradiation curves. This difference indicates that recent increases in the value of the solar constant are justified. At wavelengths longer than 4600 A, the spectroheliometer curve is slightly higher than either of the other two. This variation probably arises from location and air-mass make-up differences. In summary, the distribution curve plotted from spectroheliometer data shows good correlation with the results of others.

COMPARISON OF DETROIT AND MIAMI SUNSHINE

As previously stated, the spectroheliometer was operated in Detroit, Michigan before being put into service near Miami. Therefore, data were available with which to compare Detroit and Miami sunshine. A ratio of approximately 5 to 1 in the peak intensity of solar radation (measured at solar noon) was found to exist between Miami and Detroit, in favor of Miami. This ratio is too great to be explained either by differences in signal attenuation or by theoretical air-mass thickness. However, when in Detroit, the instrument was located near the center of this industrial area, so that air-mass make-up can explain a large portion of this intensity difference, since foreign particles present in the atmosphere are known to affect greatly the amount of radiation received.

Partially confirming this possibility, an interesting effect was noticed in Detroit that did not occur in Miami; it has been called "solar twinkle." Fig. 10 shows side by side a portion of the actual record charts for Detroit and Miami on two clear days approximately one year apart. "Solar twinkle" is an irregular periodic variation of solar radiation that occurs even on the clearest of clear days. This variation amounts on the average to approximately 16 per cent of the peak intensity of the radiation in each channel (except channel 6) and must be ascribed to the presence of unseen foreign particles in the atmosphere. Channel 6 showed no such variation because of the slow response characteristics of the pyrheliometer. From actual visual observations of the spectroheliometer recorder in Detroit, it was noted that this "solar twinkle" has a period of a few seconds. It is the over-all sampling of many of these "twinkles" that are recorded on the chart.

SUMMARY

The spectroheliometer is an instrument which monitors solar radiation from sunrise to sunset, throughout the seasons of the year. It has been used to gather a vast amount of information as to the magnitude of solar radiation reaching the earth. The ability of the spectroheliometer to produce quantitative data relating the spectral distribution of solar power and energy in an almost continuous manner is the outstanding feature of the instrument and makes it especially useful in studying the variation in solar radiation and allied effects.

REFERENCES

1. Y. T. Sihvonen. *Rev. Sci. Instr.* 28: 628, 1957.
2. Parry Moon, "Proposed standard radiation curves for engineering use." *J. Franklin Inst.* 231: 583-617, Nov. 1940.
3. Ralph Stair, Russell Johnston, and Thomas C. Bagg, "Spectral distribution of energy from the sun." *J. Nat. Bur. Standards* 53: 113-119, 1954.

VOL.
2
1958

DETAILED PROCEDURE USED IN ABBOT'S METHOD OF LONG-RANGE WEATHER FORECASTING

By C. G. ABBOT

Research Associate, Smithsonian Institute

As a result of 30 years of daily observations of the solar constant, the author discovered a numerous family of regular periodic variations of solar radiation, all integrally related to the master period of 273 months. Exactly the same family of variations was found in long-interval precipitation and temperature records, hidden to cursory search by phase changes due to various atmospheric influences. In solar variation the periods have ranges of only 0.05 to 0.21 per cent of the solar constant, whereas in precipitation they range from 5 to 25 per cent of normal, and in temperature up to 5°F.

This paper describes in detail a method of forecasting precipitation and temperature which the author has evolved from this discovery. His method can be used for forecasts up to fifty years in advance, but yields only general features, such as monthly or seasonal effects, not weekly or daily changes. With the aid of Professor C. Wexler of Arizona State College, a forecast was made for Natural Bridge, Arizona, from 1950 to 1967. The results and a comparison with the event to 1957 are given in a graph.

Applications of this method to rainfall and temperature, which I made for my own satisfaction at the Washington, St. Louis, Peoria, Albany, and Charleston, S.C., stations, attracted interest in Arizona, Iowa, and Texas. I was asked to try out the method for the stations at Natural Bridge, Arizona; Omaha, Nebraska; and Brownsville, Texas, and did so. The Association for Applied Solar Energy has now asked me to describe the procedure in detail, so that others may use it if desired.

In brief, the method consists in evaluating about 25 periods in weather from tabulations of long intervals of continuous monthly records, and adding the effects of these periods. The periods used operate simultaneously and continuously and are all integral submultiples of 273 months. Most of these periods are not as yet recognized by meteorologists. They are in fact hidden by atmospheric influences so that they do not appear as regular periods merely by direct tabulation of weather records. They would never have been recognized if they had not been identical with a family of periods previously found in the sun's output of radiation.

From 1920 to 1952, the Astrophysical Observatory of the Smithsonian observed the solar constant of radiation, as far as possible daily and at several widely separated mountain stations. This quantity is the average intensity of the solar rays, as they would be observed quite outside the earth's atmosphere at mean solar distance. Expressed in heat units, we determined the solar constant to be 1.946 cal per sq cm per min. From rocket observations at high altitudes, Johnson has improved the Smithsonian estimate for extreme ultraviolet rays and has recently published a solar constant value 2.00 ± 0.04,[1] very slightly above the Smithsonian value.

The Smithsonian observations are published as daily, ten-day, monthly, and yearly mean values in Volumes 6 and 7 of the *Annals* of the Smithsonian Astrophysical Observatory. I have also published 10-day and monthly mean values in a convenient form for tabulation.[2]*

In my paper just cited, I listed and evaluated over 60 regular periods in solar variation, all belonging to a family integrally related to 273 months. They probably all exist in weather, but, omitting inconspicuous ones, I retain in my forecasting of precipitation and temperature only 27 of them. With solar radiation, these 27 periods range in amplitude only from 0.05 to 0.21 of 1 per cent of the solar constant. But, at the stations I have thus far worked with, these 27 periods range from 5 to 25 per cent of normal precipitation, and from 1° to 5°F in temperature. I do not know any theoretical explanation of why such small percentage changes in solar radiation should produce such large changes in weather. Some critics might be inclined to suggest that the changes in weather produce small errors of observation of the solar constant. But this explanation of the identity of periods in solar radiation and weather seems untenable. For in solar radiation the periods go on continuously with perfect regularity, and occur in the same phases when observed both north and south of the equator. But in the weather these periods

*Practically all Smithsonian values of the solar constant exceed 1.900 cal. I have expressed them as departures from 1.900, in percentages of the solar constant. Thus an observed solar constant value of 1.950 cal would be tabulated in my table of departures as (1.950 − 1.900)/1.946, which is 2.57 per cent of the solar constant. Dropping the decimal point as a nuisance in tabulations and in printing, the value appears as 257 in my tables. If a solar radiation period of 7 months has an amplitude of 8 in these units, as appears from Table 2 of my paper above cited,[2] we know at once that its range is 0.08 per cent of the solar constant, as, indeed, I stated in that paper.

are shifted in phase with the locality, with the seasons of the year, with the prevalence of sunspots, and with the changes in settlement of population. Such variableness in weather phases is incompatible with weather-production of constant phases in errors of solar observation.

Observations of the sun are unnecessary to my method of weather forecasting. It is only because the periods were first discovered by solar observation that they were afterwards found in the weather. But once known to exist, the weather periods are readily found and evaluated in tabulations of monthly weather records and require no further support from solar observing.

Before proceeding to describe details, I wish to emphasize that when the weather periods have been evaluated in their average amplitudes from a long series, say 1000, of tabulated monthly mean values, then a summation of the effects of all 27 periods *is a forecast, whatever interval of years it is applied to.* For in any year there are but 12 months. The behavior of the weather during these 12 months can have but 12/1000 effect on the calculated weather for that year. The 1000 months used as a basis determine the curve of that year.

I wish to say also that the long-range forecasts, determined as they are by smoothed monthly mean values, are not applicable for daily or weekly prediction of future weather and are even apt to be a month or more out of phase with observed monthly values. They are not applicable either to localities over 100 miles from the station they represent. Their value, if any, lies in mapping the country to show areas of equal departure from the normal in future years. They are in a general way applicable to the seasons. Such information, if sound, would evidently be valuable for agriculture and for other purposes. Droughts, excessive rainfall, hot or cold seasons, could be anticipated and prepared for.

DETAILED PROCEDURE, ABBOT'S FORECAST METHOD

(1) Preparation of Records

Published records give monthly normals computed as means for each month of the year from all years in which said month was observed. If one computes separately such monthly means for years when Wolf sunspot numbers are respectively above and below 20, many stations show large percentage differences, as below in Table I.

The yearly difference between SS > 20 and SS < 20 is seen to be 16 per cent. To draw the line arbitrarily at 20 Wolf numbers does not, indeed, eliminate the influence of solar activity on phases completely, but it is far better for preserving homogeneity in computations of periodic weather changes, than to ignore the effect altogether by using book values of the monthly normals.

The following dates may be used to separate SS > 20 and SS < 20 groups of months:

SS > 20:

Jul. 1857—Aug. 1865;	Mar. 1868—Apr. 1875;
Jan. 1880—Jul. 1886;	May 1891—Nov. 1898;
Jul. 1903—Mar. 1910;	Jan. 1915—Jul. 1921;
Apr. 1925—May 1931;	Mar. 1935—May 1942;
Mar. 1945—Jan. 1953;	May 1955—(May 1962)

SS < 20:

Jan. 1854—Jun. 1857;	Sep. 1865—Feb. 1868;
May 1875—Dec. 1879;	Aug. 1886—Apr. 1891;
Dec. 1898—Jun. 1903;	Apr. 1910—Dec. 1914;
Aug. 1921—Mar. 1925;	Jun. 1931—Feb. 1935;
Jun. 1942—Feb. 1945;	Feb. 1953—Apr. 1955;

In the use of tables of periods in weather for forecasting beyond 1957, it is necessary to make extrapolations from the preceding tables of dates. This is done (of course with marginal uncertainty) by averaging the intervals (given above) in months of SS > 20 and SS < 20, and assuming that future intervals will be approximately the same as these averages. The uncertainty will usually not lead to important errors of forecasts, for generally the curves representing SS > 20 and SS < 20 for the periods are similar for a given period and differ but a few months, or even not at all, in phases. I use for future dates: for SS > 20, 84 months; for SS < 20, 52 months.

It is convenient and saves mistakes in the use of periodic tables, to be computed as stated below, if all tables employ red pencil for SS > 20 and blue pencil for SS < 20. This is not, however, necessary if this measure is inconvenient to carry out with electronic computing. But it is very desirable if, at the head of each column appearing in a table, the month of beginning is clearly entered.

The march of records of temperature or of precipitation from month to month frequently leads to large jumps. In Table II, for instance, is the precipitation of 1940 and 1952 at Natural Bridge, Ariz.

Such irregularities would tend to produce improper estimates of average runs in periodic tables, even over so great an interval for averaging as a century. This error

TABLE I

Station, Natural Bridge, Arizona

Mean Precipitation, 1890 to 1956. Wolf numbers are designated "SS".

	Jan.	Feb.	Mar.	Apr.	May	June	July	Aug.	Sept.	Oct.	Nov.	Dec.	Year
SS > 20: Means	2.76	2.86	2.39	1.60	0.58	0.44	2.78	3.62	2.21	1.56	1.72	2.77	25.29
Reciprocals	362	350	418	625	1724	2272	360	276	452	641	581	361	
SS < 20: Means	229	250	234	107	46	43	269	298	173	142	197	207	21.29
Reciprocals	437	400	427	935	2174	2325	372	336	578	704	508	483	

(Decimals are not indicated after first line, which shows inches.)

TABLE II

	Jan.	Feb.	Mar.	Apr.	May	June	July	Aug.	Sept.	Oct.	Nov.	Dec.
1940	222	310	47	173	33	113	60	308	430	454	269	10
1952	317	86	547	371	0	3	315	262	257	0	464	512

would result if departures from the mean monthly values were used as obtained directly, without smoothing, from the published records. Hence I have used a 5-month smoothing process. For example: For March I use (Jan. + Feb. + Mar. + Apr. + May) ÷ 5. For April, I drop January and add June. For May, I drop February from the April function and add July.*

The next step in preparing the records is to tabulate the actually observed mean monthly values, compute their departures from the new normals, and smooth the departure as indicated above. It is preferable to use red pencil for intervals SS > 20 and blue pencil for intervals SS < 20, and to separate the intervals by red lines and blue lines used respectively where SS > 20 begins and where SS < 20 begins. A sample from records of Natural Bridge precipitation follows in Table III.

TABLE III

	Date	Obs.	% Nor.	5-mo.	
Red	1942				
	Jan.	106	38	96	
	Feb.	199	70	101	
	Mar.	90	38	58	
	Apr.	229	143	50	
	May	0	0	81	
					—Blue
Blue	June	0	0	122	
	July	96	223	133	
	1945				
	Jan.	240	105	132	
	Feb.	114	46	103	
					—Red
Red	Mar.	571	239	82	
	Apr.	34	21	61	
	May	0	0	75	
	June	0	0	152	
	July	314	113	195	

In temperature forecasting, I use plus and minus departures from the appropriate normals suited to SS > 20 or SS < 20. In preparing precipitation tables for forecast, I use percentages of normals, as given above, in the first steps, and plus and minus departures of these from 100 per cent in later steps, as will appear below.

All stations have some months when the precipitation is so high above the published normals that, if used as printed, our tabulations would not be representative of average conditions. As my method of forecasting depends on long *representative* tabulations to give the average periodicities, all values published which are above 2½ times published normals are reduced to 2½ times before the smooth values are computed.

*I am inclined hereafter to use 3-month smoothing instead of 5-month at least for stations of fairly evenly distributed rainfall and perhaps for all temperature forecasts. For it would be better, especially in droughts, to forego some smoothness for better resolving power.

(2) Number, Lengths, and Orientation of Periods

The following periods, all integral submultiples or so-called "aliquot parts" of 273 months, are employed. I give first the fraction of 273 months, then the period in months corresponding:

Fraction	Months	Fraction	Months	Fraction	Months
1/3 . . .	91	1/12 . . .	22 3/4	1/27 . . .	10 1/9
1/4 . . .	68 1/4	1/14 . . .	19 1/2	1/28 . . .	9 3/4
1/5 . . .	54 3/5	1/15 . . .	18 1/5	1/30 . . .	9 1/10
1/6 . . .	45 1/2	1/18 . . .	15 1/6	1/33 . . .	8 3/11
1/7 . . .	39	1/20 . . .	13 13/20	1/36 . . .	7 7/12
1/8 . . .	34 1/8	1/21 . . .	13	1/39 . . .	7
1/9 . . .	30 1/3	1/22 . . .	12 9/22	1/45 . . .	6 1/15
1/10 . . .	27 3/10	1/24 . . .	11 3/8	1/54 . . .	5 1/18
1/11 . . .	24 9/11	1/26 . . .	10 1/2	1/63 . . .	4 1/3

Hitherto I have been using 23 periods, and not all were exact integral fractions of 273 months. I believe better results will come by using the 27 periods stated above.

The periods 1/3, 1/7, 1/21 and 1/39 are even months. The rest have added fractions of a month, which involves additional trouble and may cause mistakes.

It is very desirable, for convenience in making forecasts, that all periods used should start at such times that an integral number of repetitions of them will end, for all the periods, with December 1949, that is with 1950 - 0. To do this, one must compute a starting date. I give an illustration. Suppose records began with 1870. There will be about (1950 — 1870) × 12 = 960 months. Now consider the period 8-3/11 months, approximately 8.273 months. There will be about 960 ÷ 8.273 = 116 repetitions, approximately, of this period up to 1950 - 0. To get the exact starting point for the period 8-3/11 months, a number less than 116 must be selected, divisible by 11. The nearest is 110. That number of repetitions of 8-3/11 requires 110 × 8-3/11 = 910 months = 75 years, 10 months. (1950 - 0) — (75 - 10) = (1874 - 2). Two months having elapsed in 1874, the starting month for the period 8-3/11 months is March, 1874. This will bring the last repetition of the period to end with December, 1949. But about 50 months would be lost from tabulation, since the published record starts, we assume, with 1870. These 50 months may be saved by counting back, and tabulating 6 repetitions of 8-3/11 months before March, 1874.

We come now to considering the accumulation of fractions of a month. Again using 8-3/11 months, approximately 8.2727 months, we may make a table of accumulation (see Table IV).

From this we see that extra months should be added at the end of columns 2, 6, 10, 13, and 17, and similarly at later columns up to 1950. Looking back behind March, 1874, the sixth preceding column should start 50 months earlier with January, 1870.

TABLE IV

Repetitions	1	2	3	4	5	6	7	8	9	10	11	12	13	14	15	16	17
Accumulation	0.27	0.55	0.82	1.09	1.36	1.64	1.91	2.18	2.45	2.73	3.00	3.27	3.55	3.82	4.09	4.36	4.64
Wasted months	—	1	—	—	—	2	—	—	—	3	—	—	4	—	—	—	5

VOL.
2
1958

Other periods have other times to add waste months to columns. Some periods are easier to arrange than 8-3/11, and it is also easier to find the starting months in order to end with December, 1949.

(3) Tabulation

I now give in Tables V and VI an actual tabulation copied from the study of precipitation at Brownsville, Texas. It concerns the periods 9-1/10 months. A graph of it follows.

(Numbers in body of table are 5-month running means of percentage normal precipitation.)

Notes on Tables V and VI

The reader will notice five cases in Tables V and VI where several values are given daggers. These values referred to dates when $SS < 20$, though the body of the table refers to $SS > 20$. The rule is to place columns of values in tables where their majority suits the sunspot numbers prevailing, even if a minority of them do not properly fall there. It will be noticed also that 15 values are starred. These values are all over 200 per cent of normal. I print the table here just as it reached me from the computer. But before using the columns of mean values (like $\Sigma \div 11$), I recomputed all the means of the line containing the starred values, arbitrarily changing each of the starred values to 180. For it is very plain that unusually large precipitation occurred in the starred months. What is desired in the mean values are values representative of average conditions. If very large values, not representative of usual conditions, are employed, the columns of mean values obtained will oft-times be very ragged, and the forecast to be made from them will be spoiled. As stated above it is better to reduce abnormally high values to 2½ times the published normals before smoothing.

When I can see the original values before they are smoothed, I substitute values 2½ times normal for all *original* values exceeding that ratio. Then the smoothed values show no such abnormalities as those just referred to.

(4) Assembly of Tabulations

Grouping of Periods

All weather influences caused by changes in solar rays are subject to lags. For instance, June and noonday are times of highest solar altitudes, but the warmest months and hours occur later. The lag is longer the longer the period of the solar radiation change. These lags are due to atmospheric conditions, and vary from locality to locality, from month to month, from times of great sunspot activity to quiet solar times, and as population and forestation change. Hence, though the family of periods integrally related to 273 months proceeds with perfect regu-

TABLE V

$SS > 20$

a_1

1871 Feb.	1874 Mar.	1880 Mar.	1883 Apr.	1884 Jan.	1893 Feb.	1896 Feb.	1905 Apr.	1906 Jan.	1908 Apr.	1909 Jan.	$\Sigma \div 11$
62	96	108	90	86	122	87	44	153	120	94	1047
62	94	52	110	58	111	62	113	146	133	48	899
54	88	68	112	73	64	53	78	113	135	87	843
58	52	180	141	77	30	53	65	153	66	117	902
62	95	188	145	79	28	47	79	118	85	108	940
59	88	203•	136	84	33	47	119	176	118	147	1100
90	129	232•	127	115	34	67	142	125	107	140	1189
104	108	203•	130	175	45	106	146	135	102	95	1226
100	115	124	96	191	46	107	173	93	105	72	1111
						117					

b_1

1872 Aug.	1873 May	1882 July	1885 July	1891 Aug.	1892 May	1894 Aug.	1895 May	1898 June	1904 July	1907 July	$\Sigma \div 11$
109	40	103	98	101	73	101	88	24	114	44	814
112	45	70	98	108	84	99	78	32	117	36	799
117	104	93	96	115	78	37	103	24	123	61	864
85	116	114	102	109	79	24	59	40	92	59	799
68	132	117	116	112	115	34	73	40	85	64	869
53	146	125	145	128	114	66	101	46	118	65	1006
44	145	116	113	126	131	63	92	41†	144	62	979
29	105	86	114	99	170	111	86	43†	159	128	1027
32	124	65	151	92	163	109	88	46†	152	118	1036
	110										

c_1

1871 Nov.	1874 Dec.	1880 Dec.	1881 Oct.	1884 Oct.	1893 Nov.	1896 Dec.	1897 Sept.	1903 Sept.	1906 Oct.		$\Sigma \div 10$
89	138	138	167	205•	72	97	100	41	100		1147
77	168	116	193	262•	81	94	100	41	48		1186
53	116	83	195	271•	95	76	66	22	53		1030
50	126	103	208•	197	67	60	102	22	73		1008
52	117	58	191	169	76	62	117	22	108		972
66	51	50	233•	209•	53	71	95	64	106		988
85	37†	68	188	149	103	85	95	65	98		973
83	49†	86	171	108	106	69	95	67	107		941
87	40†	118	116	92	117	81	52	104	75		882
		160						133			

•Values over 200 per cent of normal.

TABLE VI

a_2

1915 Feb.	1918 Feb.	1921 Mar.	1924 Mar.	1927 Apr.	1928 Jan.	1930 Apr.	1931 Jan.	1937 Feb.	1940 Feb.	1946 Mar.	1949 Mar.	Σ ÷ 12
137	79	94	93†	80	103	139	185	109	90	159	111	1149
116	108	93	101†	83	115	122	108	134	104	137	119	1133
61	118	108	93†	82	134	118	130	100	112	117	115	1073
61	116	92	94	90	133	84	61	113	120	132	137	1028
40	100	95	124	105	107	107	81	111	50	79	148	956
36	65	88†	128	68	108	149	76†	110	56	100	137	934
37	54	65†	73	87	121	149	72†	64	76	84	123	838
39	53	39†	110	106	91	221*	91†	68	88	88	93	906
88	81	59†	115	117	123	224*	94†	100	154	76	65	1080
											45	

b_2

1916 Aug.	1917 May	1920 June	1926 June	1929 July	1935 Aug.	1936 May	1938 Aug.	1939 May	1941 Aug.	1945 June	1948 June	Σ ÷ 12
117	104	88	146	172	95	132	76	175	121	102	74	1176
130	79	99	119	114	66	171	65	185	74	97	113	1093
93	77	101	115	121	103	176	85	139	107	117	100	1112
56	57	74	92	82	101	149	68	95	114	159	92	932
46	55	53	120	66	108	149	67	48	118	132	62	853
61	14	90	130	64	105	123	66	42	90	136	58	816
59	13	101	120	64	125	108	119	33	76	142	78	860
65	24	95	105	92	110	97	145	24	55	105	78	829
66	43	76	115	124	109	107	170	93	128	164	97	1077
			52						112			

c_2

1909 Oct.	1915 Nov.	1918 Nov.	1919 Sept.	1924 Dec.	1925 Sept.	1928 Oct.	1937 Nov.	1940 Nov.	1946 Dec.	1947 Sept.		Σ ÷ 11
80	72	154	159	85	146	136	104	164	61	120		1164
43	62	170	104	104	189	139	98	179	43	113		1131
42	58	156	121	129	219*	105	129	211*	57	85		1193
45	76	183	102	110	135	91	139	219*	81	107		1171
50	28	156	87	124	148	51	103	168	78	108		1001
37	27	122	61	122	174	98	108	221*	85	89		1040
35	70	168	71	83	152	102	107	199	131	90		1098
35	110	131	106	143	134	144	112	132	119	77		1130
85	105	159	113	147	171	163	104	119	102	75		1221

*Values over 200 per cent of normal.

larity in measures of the solar constant, in weather the same family of periods is affected by changes of phase, depending on the locality, the population, the sunspot frequency, and the time of the year. The *periods* are the same in weather that they are in solar radiation, but owing to complex atmospheric influences on the lags the *weather phases* are so altered from time to time that these periods are unrecognizable without a segregation of the data, governed by consideration of these modifying influences.

It is not possible to anticipate and allow for these phase changes precisely. I content myself as follows:

(a) The year divided: Jan. to Apr.; May to Aug.; Sept. to Dec.

(b) Solar activity divided: Wolf numbers > 20; Wolf numbers < 20.

(c) Secular time divided: first half of tabulated records; second half thereof. All these divisions of data hold for periods up to 15⅙ months, or 15 groupings for these periods. The segregation according to the Wolf numbers holds from 18⅕ months up to 39 months, but not the segregation for times of the year.

Hence for these longer periods there are but four divisions to a period. The secular time segregation holds beyond 39 months, two divisions each for four periods.

The grouping just indicated leads to computing many tables:

Up to 15⅙ months	$15 \times 12 = 180$ tables
Thence to 39 months	$8 \times 4 = 32$ tables
Thence to 91 months	$4 \times 2 = 8$ tables
Total	220 tables

The numerous groups used for the shortest 15 periods leads to tabulations with so few columns that the mean values of individual periods are of little weight. To remedy this defect, I assume that the forms and amplitudes of periods up to 15⅙ months in length, and in the same grouping as regards Wolf numbers, will be similar, though in different phase relations. I therefore make superposed graphs of the six tables of one period for each of the two stated conditions of sunspot activity. From inspection I am then able to shift the individual curves of the graphs to the same phase relations. Then I take a mean for all six tables and use that generalized mean in forecasting. But when using it, I must shift back the generalized mean to the proper phase, as will appear by an example later.

Fig. 1 gives an example of these shiftings in phase.

Nomenclature Used

As stated in Section 2, 27 periods, all aliquot parts of 273 months, are to be used in the forecasts. But, as just stated, these are used in several groups, depending on the length of the periods. Lags, depending on atmospheric conditions, dictated tabulations of 12 independent group-

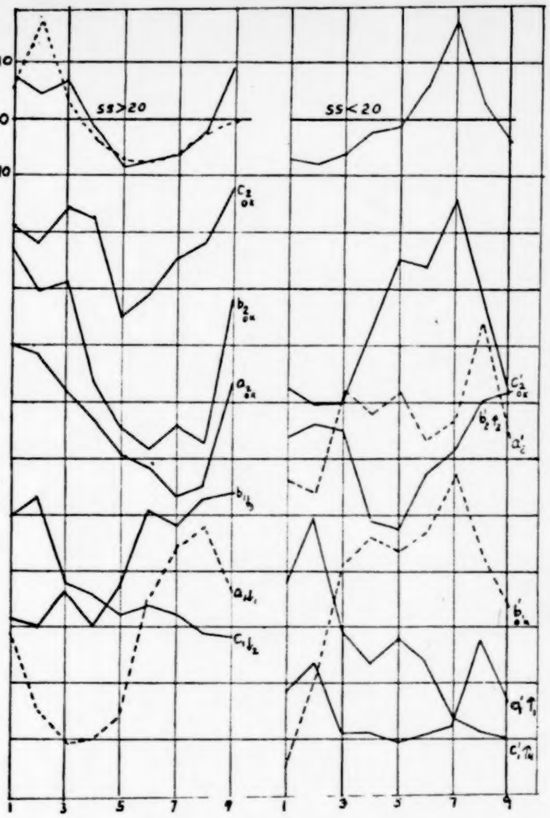

FIG. 1 — Phase shifts for combining six periods.

ings for the periods of shortest length, that is a_1, b_1, c_1, a_2, b_2, c_2, as tabulated for the period of 9-1/10 months for SS > 20 in Tables V and VI. Besides these, there are six tables, a'_1, b'_1, c'_1, a'_2, b'_2, c'_2, for SS < 20. However, for periods above 15⅙ months this extended grouping brings too few columns into the tables to be capable of yielding a satisfactory mean value. Hence for periods 273/15 to 273/7, the distinction between months of the year is dropped, thus reducing the number of groupings from 12 to 4 for these 8 periods. For the remaining 4 periods, 45½ to 91 months, the distinction SS > 20 or SS < 20 is also dropped, reducing their groupings to 2. So there are three different arrangements of assembly, as just explained, $(12 \times 15) = 180 + (8 \times 4) = 32 + (4 \times 2) = 8$, making 220 separate tabulations in all.

In the tables of periods 1/18 to 1/63 of 273 months, there are many cases when the number of columns for $a_1, b_1, c_1, a_2, b_2, c_2$, and $a'_1, b'_1, c'_1, a'_2, b'_2, c'_2$, are too few to give a trustworthy mean. Accordingly, as I stated above, I have made the assumption that in form and amplitude groups for SS > 20 will be fairly similar, though of different phases, and in form and amplitude groups for SS < 20 will also be fairly similar, though differing in phases. Making this assumption, I combine into one table $a_1b_1c_1a_2b_2c_2$, merely changing the phases to give best accord, and, similarly, I combine $a'_1b'_1c'_1a'_2b'_2c'_2$ into a single table. I give samples of this simplification here, in Tables VII and VIII, drawn in part from Tables V and VI and filled up by copying the actual computations made for period 9-1/10 months at Brownsville, Texas.

TABLE VII

9⅒-Month Period SS > 20

$a_1{\downarrow}_1$	$b_1{\downarrow}_3$	$c_1{\downarrow}_2$	a_2OK	b_2OK	c_2OK	Σ	Σ ÷ 6	Δ
1111	979	941	1149	1176	1164	6520	1085	+ 75
1049	1027	882	1133	1093	1131	6315	1053	+ 43
899	1036	1147	1073	1112	1193	6460	1075	+ 65
843	814	1180	1028	932	1171	5968	995	− 15
902	799	1030	956	853	1001	5541	923	− 87
940	864	1008	934	816	1040	5602	934	− 76
1100	799	972	838	860	1198	5667	945	− 65
1189	869	988	906	829	1130	5911	985	− 25
1226	1006	973	1080	1077	1221	6583	1097	+ 87

$$\frac{9092}{9} = 1010$$

TABLE VIII

9⅒-Month Period SS < 20

$a'_1{\uparrow}_1$	b'_1OK	$c'_1{\uparrow}_4$	$a'_2{\uparrow}_1$	$b'_2{\uparrow}_2$	c'_2OK	Σ	Σ ÷ 6	Δ′
1087	995	1179	890	1000	1024	6175	1029	− 73
961	1145	1138	1066	837	994	6141	1023	− 79
962	1360	1138	1030	853	997	6240	1040	− 62
945	1410	1014	1066	923	1121	6479	1080	− 22
961	1385	1005	980	963	1250	6544	1091	− 11
973	1418	1270	1016	1052	1236	6960	1160	+ 58
1123	1520	1391	1190	1070	1351	7645	1274	+ 172
1017	1372	1240	984	988	1178	6779	1130	+ 28
1037	1272	1134	910	1010	1010	6373	1062	− 40

$$\frac{9921}{9} = 1102$$

Combinations of a_1, b_1, c_1, a_2, b_2, c_2, and of a'_1, b'_1, c'_1, a'_2, b'_2, c'_2 for the 9-1/10-Month Period in Brownsville, Texas, Precipitation.

The phase adjustments here shown were fixed by the graph in Fig. 1. $\downarrow_n$ = moved down n places; $\uparrow_n$ = moved up n places; OK means unmoved.

The columns marked Δ and Δ′ are used in computing forecasts, as will be illustrated below. As the reader will notice, the columns Δ and Δ′ are (as wholes) in different phases. But as appears on the graph, Fig. 1, when shifted to the same phases the two determinations of the run of the 9-1/10-month period, one from observations at high solar activity, the other from observations at low solar activity, are similar. As appears from such tabulations for many periods and for many stations, the amplitudes seem to average higher for SS < 20 than for SS > 20. I show dotted at the left of Fig. 1 the curve for SS < 20, with its phase moved $\downarrow_4$. The discrepancies with the curve for SS > 20 are not large, considering the jumps even in smoothed monthly values.

Overriding Periods

Since all the periods to be used are aliquot parts of 273 months, it usually happens that a tabulation to evaluate one of the longer periods reveals in its mean one or more shorter periods, which are integral submultiples riding upon the longer period in question and preventing a true picture of the form and amplitude of the period sought to be evaluated. When several such submultiple periods are superposed, it is often difficult to know how to remove them or even to know which of the shorter periods, which might be integrally related to

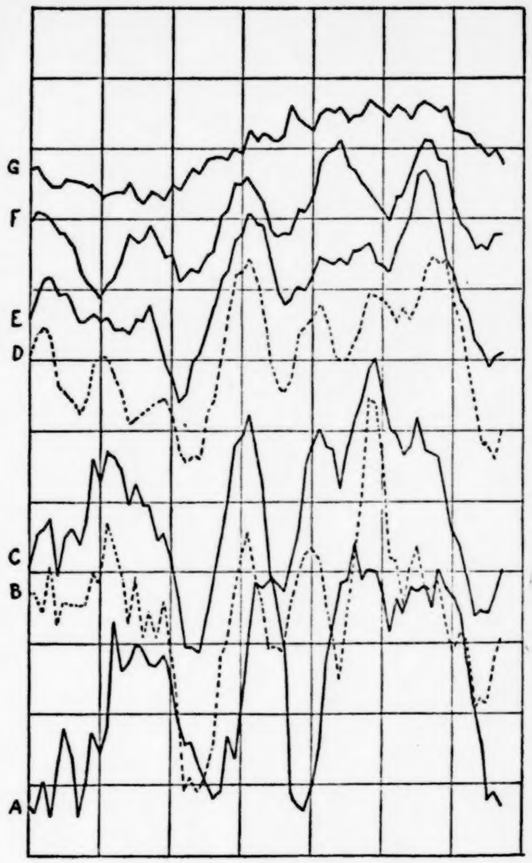

FIG. 2 — The 68½-month period in St. Louis precipitation cleared of shorter integrally related periods.

their host period, are present.

Having computed the mean value of the many columns tabulated for the long period, we graph this mean value. Fig. 2 shows one such graph, Fig. 3a another. By inspection, the most probable subordinate overriding period is chosen. Its length will usually be from ½ to ⅛ of the length of the graph. Each of its humps is then tabulated as one column of a table made to determine their average form and amplitude. If a good curve results, its average ordinates are subtracted from those of the longer curve, and the result graphed. This second graph is treated similarly, and so on to others, until only the fairly smooth curve representing the long period in question remains.

As a graphical illustration, I reproduce here as Fig. 2, Fig. 9 of my paper "Sixty-year Weather Forecasts."[3] It represents the evaluation of the 68½-month period in St. Louis precipitation. A and B are mean curves, A of 8 repetitions prior to 1900, and B of 7 repetitions subsequent to 1900. The phase of A appears to be 3 months later than the phase of B. Moving A back 3 months and taking the mean of the two, curve C results. This shows plainly the presence of a period of ⅓ of 68½ months. Obtaining its average form and amplitude and subtracting from curve C, curve D is obtained. Curve D presents 7 humps of about equal length. Taking their mean form and amplitude and subtracting, curve E remains. In curve E halves are clearly indicated, though not exclusively. Evaluating the average half and subtracting, curve F appears. And now obviously there remains a regular period of ⅕ of 68½ months. Evaluating and subtracting, we find curve G, which well represents the 68½-month period sought. Its range is 13 per cent of St. Louis normal precipitation. This single diagram presents five members of the family related integrally to 273 months. These are 1/4, 1/8, 1/12, 1/20, and 1/28 of 273 months.

In Figs. 3a and 3b are given the results and details of the removal of overriding periods from the curve of the period of 45½ months in the precipitation at Natural Bridge, Arizona, for SS < 20, between the years 1890 and 1920. In curve A_1 are the average values of the precipitation for all repetitions of the 45½ month period when SS < 20. Curve Δ_1 remains after the removal of the average ordinates of the period (45½)/4 months. Curve Δ_2 is what remains after removing from curve *B* (45½)/6 months. Curve Δ_3 remains after removing (45½)/7 months. Curve Δ_4 remains after removing (45½)/5 months. Curve Δ_5 remains after removing (45½)/3 months, and it shows approximately the true form of the 45½-month period. The amplitude of the smooth curve through curve Δ_5 is 21 per cent of normal precipitation at Natural Bridge. The reader should understand that in three other cases the 45½-month period was similarly cleared of overriders. These cases are for SS$<$20, in the years 1921 to 1950; for SS > 20, between 1890 and 1920; and for SS > 20 from 1921 to 1950. So this one period, 45½ months, involved much thought and work, requiring three treatments similar to Figs. 3a and b. All the periods above 22 months in length required them also.

A curious algebraic theorem affords a useful check on the figures, when a long period is being divested of an overrider of one-half of its length.

Let a periodic curve be represented by equally spaced ordinates *a, b, c . . . k, l, m,* and proceeding further, *n, o, p . . . x, y, z.*

The mean form of the supposed overriding period of one-half length is:

$$\frac{a+n}{2}, \frac{b+o}{2}, \frac{c+p}{2} \ldots \frac{k+x}{2}, \frac{l+y}{2}, \frac{m+z}{2}$$

When this half-length curve is written twice, and subtracted, we have:

$$\frac{a-n}{2}, \frac{b-o}{2}, \frac{c-p}{2} \ldots \frac{k-x}{2}, \frac{l-y}{2}, \frac{m-z}{2}$$

and following that:

$$\frac{n-a}{2}, \frac{o-b}{2}, \frac{p-c}{2} \ldots \frac{x-k}{2}, \frac{y-l}{2}, \frac{z-m}{2}$$

So the last half of the long curve, when cleared of the period of one-half of its length, is exactly like the first half, but with reversed signs. This curious result enables the computer to make a check on his work.

Merely referring to the two examples given above, of the clearing of overriders of lesser length integrally related

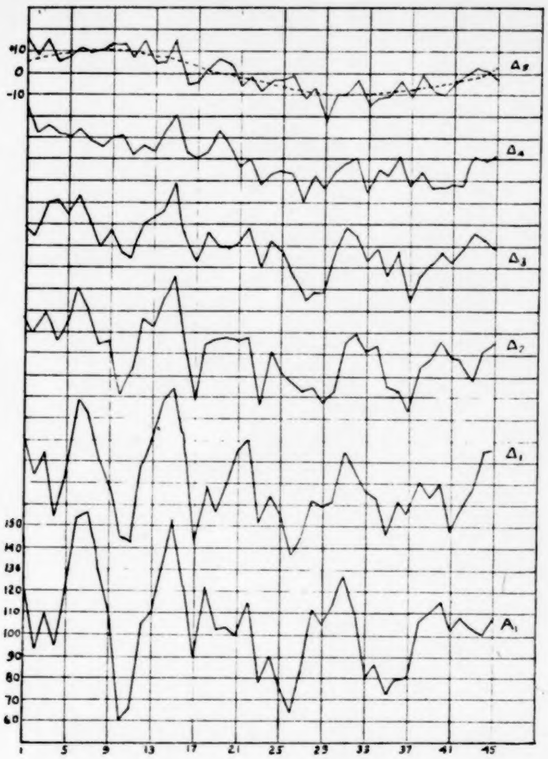

FIG. 3a — The 45½-month period in Natural Bridge precipitation, between 1890 and 1920, for intervals of Wolf numbers below 20, cleared of shorter integrally related periods.

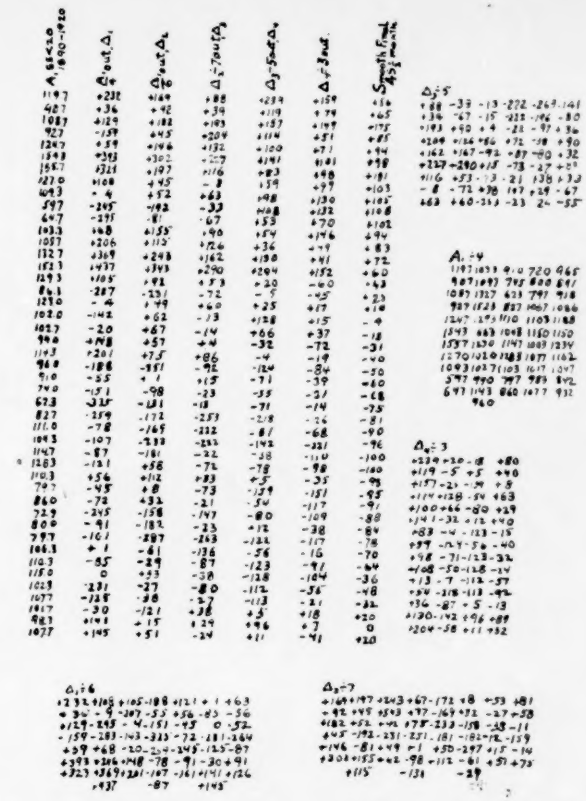

FIG. 3b — Detailed values used in graph, Fig. 3a, including subordinate period determinations.

to the original periodic curves, the reader has proof that not less than 11 integral submultiples of 273 months exist as regular periods in precipitation. Those discovered are 1/4, 1/6, 1/8, 1/12, 1/18, 1/20, 1/24, 1/28, 1/30, 1/36, and 1/42 of 273 months. Their ranges in no case are less than 10 per cent of normal precipitation. Yet, as stated above, all of them are as yet unrecognized by meteorologists.

(5) Forecasting

When tabulation of the 27 periods named in Section 2 is completed, a forecast may be made by summing their contributions, assembled in proper phase relations in 27 columns. Such a forecast may be computed for any interval of time, whether before, within, or after the interval used to tabulate and determine the periods. For during any one year there are but 12 months, while each period is to be tabulated by the use of a thousand months, more or less. So the form and range of the weather element during any one year depends on some 1000 months of records, and this year itself can contribute no more than 12 of them. Its own records can have, at most, only 12/1000 or 1.2 per cent influence on the forecast. In other words, a bona fide forecast can extend, not only from the beginning to the end of the long interval of years on which it is based, but also to years preceding and years following the interval which is the base of the forecast.

It will be noted in the combined tabulation, illustrated in Fig. 1, that the columns $a_1b_1c_1a_2b_2c_2$, $a'_1b'_1c'_1a'_2b'_2c'_2$ are apt to be displaced in their phases in computing the general mean march for a period. When this general mean march is tabulated for forecasting, these phase shifts must be reversed. For if the general mean march Δ is used, for instance, where $a_1\downarrow_1$ of Table VII would properly fall, the whole column Δ must be raised up one month, because $a_1\downarrow_1$ was lowered one month in the determination of Δ. And similarly for all other combined tables. Also, if a forecast is to be started at some year other than 1950, when all the periods were arranged in harmonious phase, a computation similar to that in Section 2 must be made for each period. Then the period will be started at the proper month to be in correct phase relations with all of the other periods.

Another point to be attended to: Most of the periods used are not *even* months long, and months have been wasted at various intervals, as shown in several illustrations above. It must be arranged, when writing periodic data into the forecasting tabulation, that these same wasted months, as the periods repeat, shall have each its vacancy at the proper month in the column used for forecasting. Such vacancies are to be filled by ordinary interpolation. As illustrated in Section II, the positions of vacant months follow predetermined courses.

TABLE IX

1875	$4\frac{1}{6}$	$5\frac{1}{18}$	$6\frac{1}{16}$	7	$7\frac{7}{12}$	$8\frac{8}{11}$	$9\frac{1}{10}$	$9\frac{3}{4}$	$10\frac{1}{6}$	$10\frac{1}{2}$	$11\frac{1}{4}$	$12\frac{11}{22}$	13	$13\frac{13}{20}$	$15\frac{1}{8}$	$18\frac{1}{6}$	$19\frac{1}{2}$	$22\frac{3}{4}$	$24\frac{8}{11}$	$27\frac{3}{10}$	$30\frac{1}{6}$	$34\frac{1}{4}$	39	$45\frac{1}{2}$	$54\frac{3}{8}$	$68\frac{1}{4}$	91	Σ	Obs.	Fore-cast
Jan.	+12	−23	−20	− 3		−14	+ 61	− 11	+21	+ 3	−31		−60	−41	−52			−45	− 93		−45	+ 73	+ 48	−11	−30	+42	+70	−205	76	80
Feb.	+13	−33	−33	−36		−34	− 77	− 52	+12	+13	−86		+10	−17	− 8			−61	−103		−38	+ 69	+ 96	−12	−44	+45	+65	−324	73	68
Mar.	−30	− 4	−26	−18		−26	− 58	−101	+21	+51	−54		−17	+ 7	+ 6			−76	− 56		−30	+ 30	+150	−17	−30	+48	+65	− 94	86	91
Apr.	+ 4	− 2	−13	+52		−18	0	− 52	+15	+69	+ 7		+42	+50	+35			−80	− 4		−15	+ 89	+135	−21	− 5	+50	+62	+338	126	134
May	+ 4	+14	− 2	+29		− 9	+ 44	− 6	−14	+45	+31		+29	+95	+38			−55	+ 9		− 3	+ 93	+115	−28	+ 5	+53	+60	+522	150	152
Jun.	+12	+26	−32	+32		+ 3	+ 61	+ 15	−41	−15	+26		+25	+45	+19			−39	+ 21		+15	+ 99	+102	−21	+30	+55	+69	+496	144	150
Jul.	+13	+14	−26	−18		+18	+108	+ 91	−18	−14	+30		+29	−11	+ 6			−22	+ 78		+30	+111	+ 93	−36	+49	+57	+57	+642	141	164
Aug.	−30	+26	+43	−38		+84	+ 7	+111	−29	−47	−11		+41	−29	+35			+ 4	+ 82		+47	+ 27	+ 75	−32	+52	+58	+54	+649	141	165
Sep.	− 8	−33	+49	−36		− 9	− 30	+ 32	−15	−20	−31		+24	+ 8	+28			+12	+ 72		+55	+ 79	+ 66	−32	+45	+60	+53	+405	120	140
Oct.	+15	− 4	+46	−18		+ 3	− 53	− 17	−16	+ 2	−86		− 2	−53	+19			+25	+ 57		+30	+ 50	+ 54	−31	+38	+62	+46	+263	150	126
Nov.	−30	− 2	+49	+52		+16	+ 44	+ 15	+57	+13	−54		−46	−92	+34			+33	+ 43		+70	+ 44	+ 44	−30	+30	+63	+44	+452	163	145
Dec.	+ 4	− 4	+49	+27		+39	+ 61	+ 91	+40	+51	+ 7		−50	−62	+42			+49	+ 18		+92	+ 25	+ 34	−24	+21	+64	+42	+674	173	167
1876																														
Jan.	+12	− 2	−13	+32		−14	+108	+111	+15	+69	+31		−56	−41	+40			+64	+ 33		+80	+ 21	+ 25	−28	+13	+63	+39	+683	140	168
Feb.	+12	+14	−20	−18		+ 4	+ 7	+ 32	−14	+45	+26		−60	−17	+25			+77	− 3		+63	+ 4	+ 17	−35	+10	+62	+36	+307	130	131

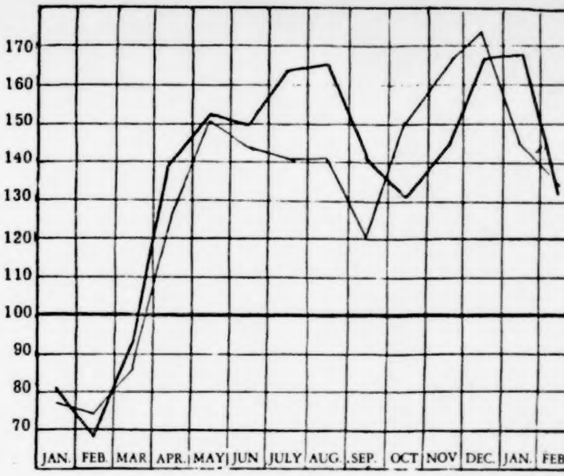

FIG. 4 — Specimen forecast of precipitation at St. Louis, 1875 to 1876. Thick line is forecast, thin line observed value.

We are apt to avoid mistakes if each column is inconspicuously marked in advance at its side to show when the periods start at zero phase, where each repetition ends, and where the vacancies occur. The sheet should also be ruled across with blue pencil to show where SS changes from > 20 to < 20 and with red pencil to show where the change comes from SS < 20 to SS > 20.

In tabulating the long columns for forecasting, careful attention is required, especiallly for the 15 periods which are represented by mean values of 6 determinations $a_1b_1c_1a_2b_2c_2$. A shift of phase is usually necessary at the end of each period entered. When passing over a change in solar activity, SS > 20 or SS < 20, one part of a period may be from $a_1b_1c_1a_2b_2c_2$, and another from $a'_1b'_1c'_1a'_2b'_2c'_2$. Every recurrence of a wasted month must have its vacancy for all the periods. Plus and minus signs must be used as they recur.

In Table IX, I give a specimen forecast from St. Louis precipitation which appeared in my paper "Sixty-year Weather Forecasts."[4] The practices I now recommend differ slightly from those followed in 1955. I have thought it better for the present purpose to print the present choice of periods and the presently used dates of passing from SS > 20 to SS < 20, rather than those actually used in the St. Louis forecast. As for the date of change of sunspot frequency, I formerly used January, 1875, rather than May, as indicated here. The run of Wolf numbers in 1875 goes:

Jan. 14.6; Feb. 22.2; Mar. 33.8; Apr. 29.1; May 11.5.

This illustrates one aspect of the impossibility of perfect precision in my attempt to work out a method of long-range forecasting. But I feel that the results obtained at a considerable number of stations justify even so rough a method as mine. I show in Fig. 4 how nearly this excerpt from the St. Louis forecast agrees in major features with the event. The average deviation between forecast and event during these 14 months is 5 per cent of normal St. Louis precipitation. The range of 5-month smoothed precipitation during that interval is 100 per cent of normal precipitation. The mean epoch of the 84-year basis, 1856

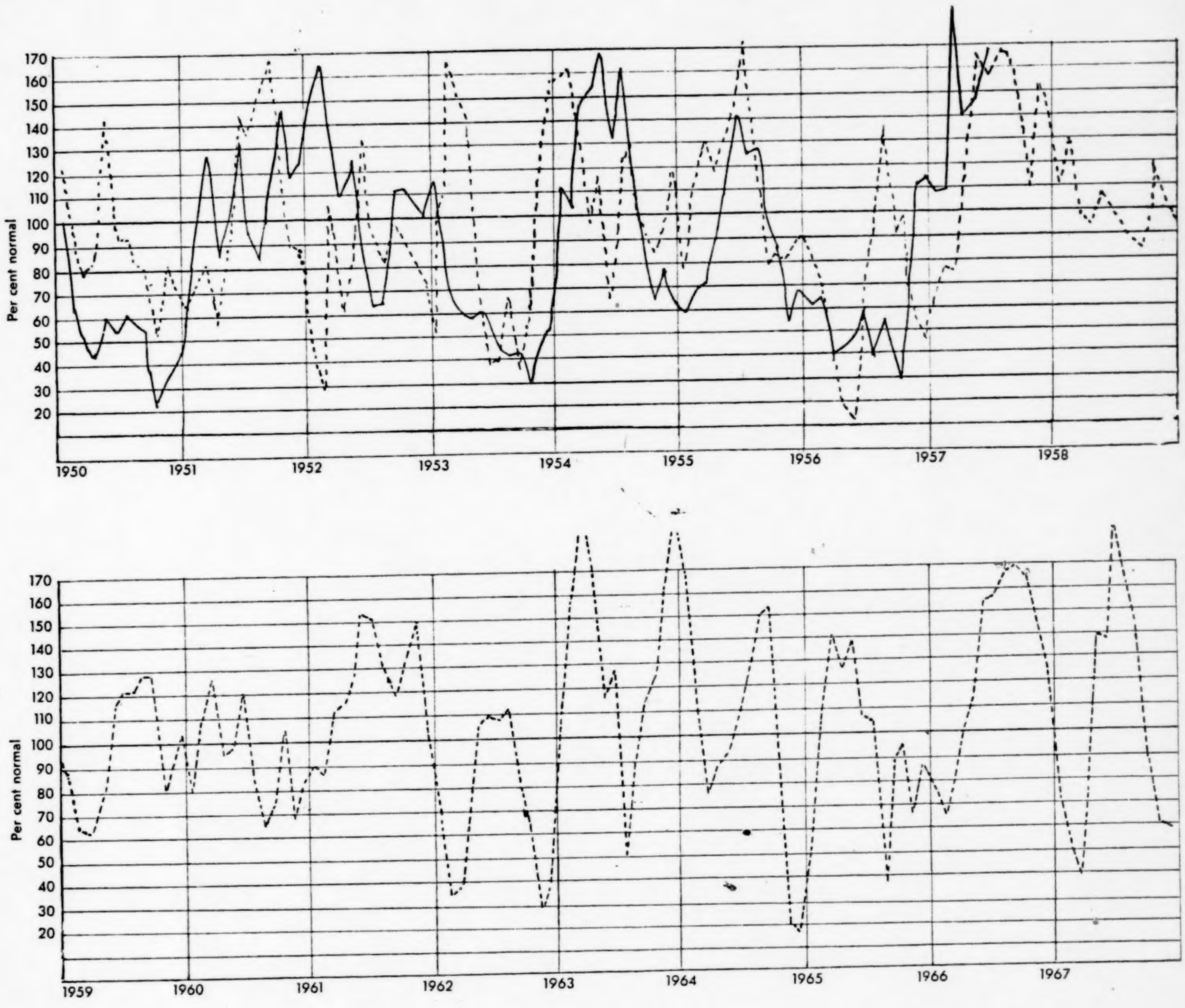

FIG. 5 — Forecast for Natural Bridge, Arizona; Precipitation, 1950-1967.

Solid line is observed value, dotted line forecast.

to 1939, used to determine the form and range of periods for forecasting is 1898. So the forecast shown is 23 years from its base.

(6) Precipitation at Natural Bridge, Arizona

While attending the symposium on solar radiation at Phoenix, Arizona, in November 1955, I was informed that the rainfall had been decreasing in Arizona during the past half century. It was suggested that I attempt a long-range forecast, to see if this trend was likely to continue. My previous tests of my method had all been for stations east of the Mississippi, where comparatively uniform precipitation comes all through the year. I feared that in more arid regions, where precipitation is more irregular, the method would fail. However, after inspecting the records of all the Arizona Weather Bureau stations, it seemed worth while to try Natural Bridge, not far from Flagstaff, in the central part of the state. With only one month lost, the record there is continuous since 1890, and by no means as irregular as at most Arizona stations.

The necessary tabulations were performed under the direction of Professor C. Wexler of the Arizona State College at Tempe, employing, for the first time in my work, the electronic computer. In that way I was furnished with 186 tables of precipitation, with their mean values attached. It required about two weeks of my time for plotting, for averaging of 156 tables in groups of six, for clearing about ten periods from overriding periods integrally related, and finally for computing a forecast for 18 years, 1950 to 1967.

Observed precipitation was available for comparison up to the middle of 1957. Though the agreement with my forecast is not so good as found for more regularly watered stations like St. Louis, there is yet enough general agreement between forecast and event for 8 years to warrant the hope that the forecast will correspond roughly to the trend of precipitation up to 1967. If so, it will appear that, except in the years 1962 and 1965, the rainfall of Central Arizona is likely to be, on an average, at least up to the average precipitation from 1890 to 1949. The dry years 1950, 1953, and 1956 corresponded to dry forecasts, but 1952 was forecasted to be much dryer than the event proved. Readers should recall that in the accompanying Fig. 5 the curves represent 5-month smoothed monthly values both in the forecast and the event.

REFERENCES

1. *J. Meteor.* 2(6), Dec. 1954.
2. *Smiths. Misc. Coll.* 117(10), Table 4, and *Ibid.* 128(4), Table 1.
3. *Smiths. Misc. Coll.* 128(3): 17, 1955.
4. *Smiths. Misc. Coll.* 128(3), 1955.

COMPUTATION OF ABSORBER AREA

By J. CL. DE BREMAECKER

Institut pour la Recherche Scientifique en Afrique Centrale (I.R.S.A.C).
Lwiro, Bukavu, Belgian Congo

From the daily data for global radiation, the value of the amortizement, the cost of the auxiliary power, and the cost of the unit area of absorber, it is possible to find the size of the absorber that will result in a minimum yearly cost. An example from Africa for the daily heating of 55 gal shows that after an initial outlay of $250 the yearly electricity bill is about $81.

For most of the uses of solar energy, one of the prime requirements is the ability to compute the area of the absorber in such a way as to minimize the cost of operating the installation. With few exceptions this seems to have been done either by hit and miss processes or at least with very little use of the solar radiation data now widely available.

Qualitatively, it is clear that, all other factors being unchanged, a smaller absorber will be needed if the radiation is intense; similarly, if the absorber is expensive, a smaller one will have to be used; and finally, if the auxiliary power is expensive, the absorber will have to be larger. The problem is how to find the balance between these various factors.

Quantitatively, the yearly cost of a system using solar energy is the sum of the interest on the investment, the yearly maintenance of the installation, the yearly depreciation, and the cost of the auxiliary power.

Thus, the question is how to compute the area of an absorber designed to meet the following specifications:

(1) output: at least Q kcal per day,
(2) cost: k \$ per sq m,
(3) cost of auxiliary power: z \$ per kcal,
(4) over-all efficiency: y.

Further, let:

E be the number of kcal per sq m per day on a horizontal area (global radiation),
N, the area of the absorber in sq m,
b, the cost of the part of the apparatus which is independent of the size of the absorber (tank, insulation, pipes, etc.).

The price P of the unit will then be

$$P = kN + b \qquad [1]$$

Now let:

i be the interest on the capital invested,
e, the cost of yearly maintenance expressed as per cent of the price,
d, the life expectancy of the unit.

The yearly cost of the unit not counting any outside power is thus:

$$C_1 = a(kN + b) \qquad [2]$$

where

$$a = i + e + (1/d) \qquad [3]$$

I will call a the amortizement factor.

Now let S be the deficit in kcal per sq m of absorber area, which has to be supplemented by outside power. The yearly cost of outside power will be

$$C_2 = zSN \qquad [4]$$

Hence, the total yearly cost will be

$$C = C_1 + C_2 = a(kN + b) + zSN \qquad [5]$$

S can now be computed as follows:

First E is plotted in order of increasing values against the days of the year, i.e., a histogram of E is made (Fig. 1). If the area of the absorber is such that it will collect sufficient heat when the number of kcal per sq m per day is greater than E_n, then the total hachured area will represent the number of calories that will have to be supplied by an outside source for each square meter of absorber. Let this deficit in calories be S and let it be plotted versus E. In most cases the computation of S can be made by dividing E in steps of 250 and by counting the number of days in each step. This is done for one year. If data are available for more than one year, average values should be taken.

Then let:

D_i be the number of days in the step for which

$$\overline{E_i} - (h/2) < E < \overline{E_i} + (h/2),$$

(In the figure, $D_i = 11, \overline{E_i} = 2375$)

h be the height of the step (here 250),
S_n be the deficit to be furnished by outside power.

Hence

$$S_n = S_{n-1} + h \sum_{i=1}^{n-1} D_i \qquad [6]$$

with

$$S_1 = 0.$$

In practice this is a very easy computation; Table I gives an example based on the values found at Lwiro in 1953.

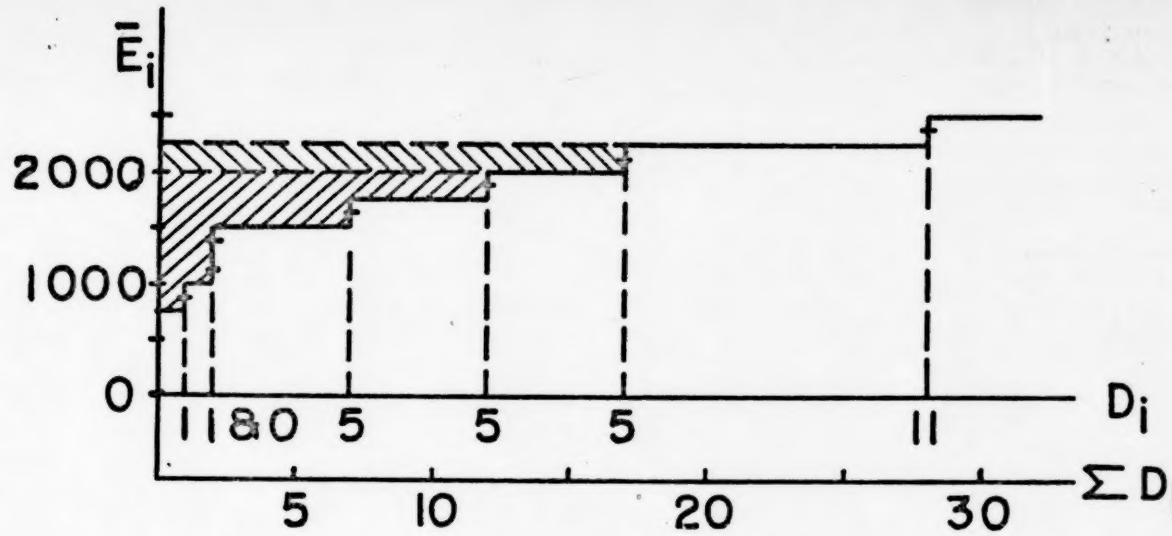

FIG. 1 — Approximation to histogram of E versus ΣD_i by steps of 250. Lower hachured area: S_{n-1}; total hachured area: S_n.

TABLE I

n	Limits of E	$\overline{E_i}$	D_i	$\sum_{i=1}^{n-1} D_i$	S_n
1	500 — 750	625	0	0	0
2	750 — 1000	875	1	0	0
3	1000 — 1250	1125	1	1	250
4	1250 — 1500	1375	0	2	750
5	1500 — 1750	1625	5	2	1250
6	1750 — 2000	1875	5	7	3000
7	2000 — 2250	2125	5	12	6000
8	2250 — 2500	2375	11	17	10,250

It is possible, from these developments, to compute the cost for various absorber areas and various prices per unit area, but this is a fairly awkward method. It is easier to express S as a function of $\overline{E}$, hereafter written E for simplicity. In all the cases that have been investigated so far, an equation of the form

$$S = \frac{pE^2 + rE + m}{qE + 1} \qquad [7]$$

is a good approximation. The important values of E are those between 1000 and 5000.

If we select one particular value of E for which we desire the absorber to be sufficient, then, for this value, the area to be selected is:

$$N = \frac{Q}{yE} \qquad [8]$$

and hence the total yearly cost is

$$C = a\left[\frac{kQ}{yE} + b\right] + \frac{z\,(pE^2 + rE + m\,)Q}{(qE + 1)\;yE} \qquad [9]$$

The problem is to minimize C, i.e., make the partial derivative of C with respect to E equal to O. This yields the best value of E, say E_o. After some computations one finds:

$$E_o = \frac{q\,(ak + zm) + \sqrt{(ak + zm)\,z\,\{p + q\,(\,mq - r)\}}}{z\,(p - rq) - akq^2} \qquad [10]$$

(Another algebraic solution exists with a minus sign before the square root. It is negative and has no physical meaning.)

This result shows that the best value of E depends neither on the number of calories desired (Q), nor on the efficiency (y), nor on the fixed investment (b), but only on the cost of the unit area of the absorber (k), the value of the amortisement factor (a), and the local radiation, which determines S as a function of E, and hence m,p,q and r.

From this value E_o one can find all the desired quantities. If Q and y are known, the area N_o follows from [8], the price P_o from [1] for any k and b, the yearly cost from [5], etc.

It turns out that the curve giving C versus N is very flat for N up to 10 per cent smaller than N_o, but fairly steep for values larger than N_o. If thus a choice is to be made between two sizes slightly different from N_o, it recommended that the smaller one be selected.

A very simple example follows: In Lwiro (Belgian Congo), very accurate solar radiation data were available for 1953, by courtesy of Mr. G. Bonnet, Solar Radiation Laboratory, I.R.S.A.C. Table I is based on these data. This table was extended up to $\overline{E} = 5375$. From it the following values were found for the coefficients of Equation [7]:

$$m = 4336 \qquad q = -\,191.41 \times 10^{-6}$$
$$p = 3.756 \times 10^{-3} \qquad r = -\,8.242$$

by fitting the curve through the points corresponding to $\overline{E}$ = 875, 1625, 2625, and 3875. It is recommended that these same values of E be used in any similar work to facilitate comparison.

A simple water heater was built, suited to local African conditions; the absorber price (k) was \$30 per sq m; the amortizement factor (a) was taken as 0.1; the cost of electricity was 6¢ per kwh. Using these data one finds $E_o = 2415$ from [10].

It was desired to heat 200 1 (55 gal) a day from 15° to 60°C, hence Q = 9,000 kcal per day. The efficiency was

estimated as 0.6. Hence, the absorber area, $N = 6.20\ m^2$ from [8]. By using a 55-gal oil drum insulated with treated wood shavings, the price of the tank and piping *(b)* was kept down to $80. Hence:

The price of the unit $P = \$266$ from [1].

The yearly electricity bill $C_2 = \$5$ from [4].

The total yearly cost $C = \$32$ from [5].

By comparison, an electric water heater of the same capacity costs about $110 in the United States and about $200 in Lwiro. If it heats only 150 l per day at 6¢ per kwh, the yearly electricity bill will be $172 (instead of $5), and the total yearly cost will be $192 (instead of $32). It is clear that the tank of a commercial heater is much more expensive and durable than the one used; hence the comparison is not straightforward. Nevertheless, the example shows that in some underdeveloped countries the solar heating of water is an economic proposition.

CONCLUSIONS

By using data for the daily global radiation now widely available, it is possible to find the optimum balance between the size of the absorber, its cost per unit area, and the cost of auxiliary power. An example from Africa shows that the yearly electricity bill is about $5 after an initial total outlay of $270.

BIBLIOGRAPHY

De Bremaecker, J. Cl., "Chauffe-eaux solaires." *Bull. Acad. Roy. Sci. Col.* 2(3): 462-76, 1956.

——"Réalisation d'un chauffe-eau solaire." *Fol. Sci. Afr. Cent.* 3(2), 1957.

Hawkins, H. M., "Domestic solar water heating in Florida." *Florida Eng. & Ind. Exp. Sta., Bull.* 18, 1947.

Morse, R. N., "Solar water heaters for domestic and farm use." *C.S.I.R.O., Melbourne, Eng. Sect., Rept.* E.D. 3, 1956.

——"Solar water heaters for domestic and farm use." *C.S.I.R.O., Melbourne, Eng. Sect., Rept.* E.D. 3, suppl., 1957.

Stewart, S. A., "Solar heating for married quarters." *J. Roy. Engr.* 70(1), 1956.

CARBON DIOXIDE SURGES IN GREEN LEAVES

By JOHN P. DECKER and JANET D. WIEN*

Rocky Mountain Forest and Range Experiment Station, Forest Service, U.S. Department of Agriculture**

CO_2 concentration of a fixed volume of air surrounding a eucalyptus leaf was measured continuously by an infrared gas analyzer while the leaf was alternately illuminated and darkened. A brief insurge of CO_2 was recorded during the initial few seconds of illumination, and a matching outsurge when the leaf was darkened. The surges appear to result from lags between rate changes of photosynthesis* and respiration.*****

CO_2 evolution from the leaves of tobacco and several other plants, as measured with the highly specific infrared gas analyzer, has been reported as very rapid during the first several seconds of darkness immediately following a period of illumination.[1] Gaffron and Rosenberg[3] have reported a similar outsurge from the alga, *Scenedesmus*. Several workers have reported phenomena that suggest initial insurges or initial outsurges of CO_2. These works were reviewed by Rabinowitch.[5]

Kok and Spruit,[4] using *Chlorella* in a volumeter, observed a rapid outsurge of gas immediately following darkening and a matching insurge at the beginning of illumination. However, they stated, "An unambiguous assignment of any transitory effect to a particular gas is not possible with manometric or volumetric methods." The nature of these latter surges is not clear, because simultaneous potentiometric (CO_2) and polarographic (O_2) studies did not confirm their existence.

In studies reported here, initial insurges of CO_2 upon illumination as well as outsurges upon darkening were observed with intact leaves of eucalyptus (*Eucalyptus* sp.) and to a lesser extent with Freemont cottonwood (*Populus fremontii*).

METHODS AND MATERIALS

CO_2 uptake and evolution were measured as changes of CO_2 concentration of a fixed volume of air surrounding a single leaf. The apparatus was essentially as described before.[1] It consisted of a leaf chamber, an air pump, and an infrared gas analyzer (Liston-Becker model 15, coupled to an Esterline-Angus recording milliammeter) connected in closed series with plastic tubing and ground glass joints. The leaf chamber was the top of a 9.5-cm Petri dish sealed to a horizontal base plate with modeling clay. Air temperature in the chamber was held within $\pm$ 0.5° by automatic control of the flow of tap water through loops of copper tubing soldered to the underside of the base plate. The thermoregulator was an ordinary mercurial thermometer to which was attached a Thermocap relay that controlled a solenoid valve. Illumination was provided by a 150-watt internal-reflector floodlamp directed downward onto the chamber through a heat filter of 30 mm of cold water. The vertical wall of the Petri dish was covered with black opaque tape so that the leaf could be darkened quickly and completely by covering the chamber with a flat piece of cardboard.

The eucalyptus plants were potted seedlings about 100 cm tall purchased from a commercial ornamental nursery. The cottonwood leaves were on branches about 150 cm long cut from fully exposed parts of mature ornamental trees. The branches were recut under water immediately, and the cut ends were kept in water throughout the experiments.

SURGES

The routine operating procedure was as follows. An intact leaf, still attached to a branch, was sealed in the chamber and left for 30 minutes at 30°C and 2200 fc and with laboratory air passing through the chamber at about 1000 ml per minute. Then a slight excess of CO_2 was added to raise the concentration conveniently above 400 ppm, and the system was closed and recordings were made of the changes of CO_2 concentration through repeated light-dark-light cycles.

Fig. 1 is a direct copy of a record made while a eucalyptus leaf was exposed to a light-dark-light cycle at 30°C. The cycle was repeated 166 times at this temperature, using 12 leaves of 6 plants. There were 166 distinct outsurges and 164 distinct insurges. During 111 cycles at 40° there were 97 outsurges and 101 insurges. During 70 cycles at 20° there were 70 outsurges and 70 insurges.

The delay of about 7 seconds between a change of light intensity and a change of direction of the tracing is

*Present address: Botany Department, Arizona State College, Tempe, Arizona.

**Central headquarters maintained in cooperation with Colorado State University at Fort Collins, Colorado; research done at Tempe, Arizona in cooperation with the Arizona State College.

***For simplicity of expression, arbitrary definitions have been assigned to several terms used in this paper. Total CO_2 consumption (from both internal and external sources) is designated as photosynthesis. Total CO_2 production is designated as respiration. This usage implies nothing as to any component process of either and nothing as to oxygen exchange. Measurable decrease and increase of CO_2 concentration in the system surrounding the leaf are designated as CO_2 uptake and evolution, respectively.

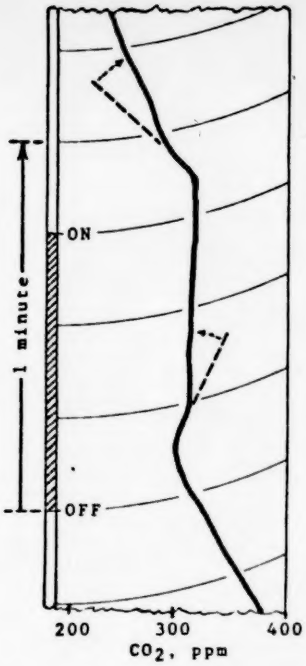

FIG. 1 — Portion of milliammeter chart showing changes of CO_2 concentration in system when a eucalyptus leaf was exposed to alternate 45-second periods of dark and light. Rates of decrease and increase of CO_2 are measures of rates of CO_2 uptake (apparent photosynthesis) and CO_2 evolution, respectively. Extension lines emphasize differences between momentary rates (surges) and subsequent steady rates. Angles indicated are measures of the differences.

FIG. 2 — Similar to Fig. 1. Cottonwood leaf. Note lack of initial surges compared to Fig. 1.

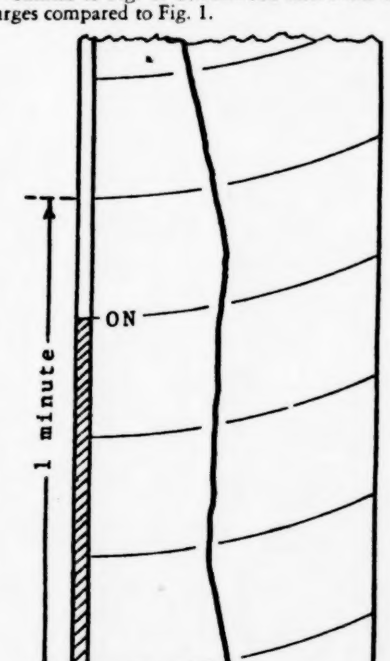

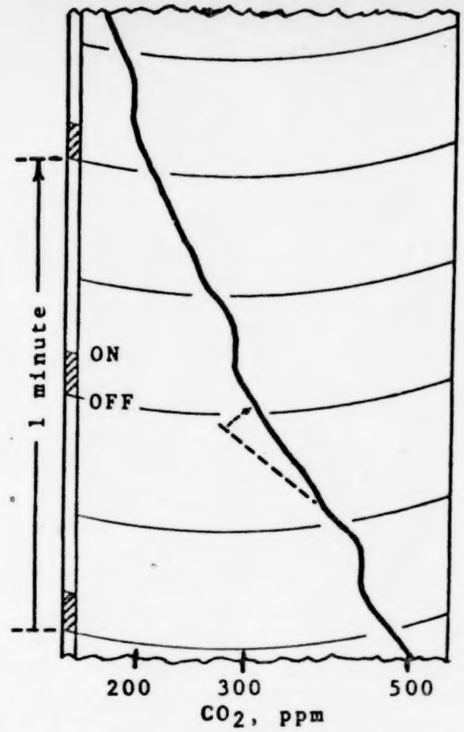

FIG. 3 — Similar to Fig. 1. Eucalyptus leaf exposed to 5-second dark periods alternated with 25-second light periods.

largely instrumental lag. In preliminary work when a burst of CO_2 was injected directly into the chamber with a microsyringe, the meter indicated the change of concentration about 6-8 seconds later.

Eight cottonwood leaves were subjected to repeated light-dark-light cycles at 30°. Two showed insurges and outsurges distinctly and consistently. Six gave no evidence of surging, as shown in Fig. 2. No test was made to determine whether the lack of surging was a characteristic of the species or the result of injury from cutting the branches.

A preliminary study was made of the effect of length of light and dark periods on surging. A eucalyptus leaf was subjected to a series of light-dark-light cycles at 30° with the dark period shortened to 5, 2, or 1 seconds. Fig. 3 shows the insurge following 5 seconds of darkness. This record is practically identical with 12 others (65 cycles) made in rapid succession. Fifty-five cycles were run with the same leaf with a 2-second dark period and 45 cycles with a 1-second. Insurges were diminished but were distinct on all records.

The same leaf was subjected to a series of dark-light-dark cycles at 30° with the light period shortened to 5, 2, or 1 seconds. Outsurge was never evident following 1 or 2 seconds of light and was barely discernible following 5 seconds.

In considering hypothetical explanations for the surging, one obvious possibility is an increased respiration during illumination, with its acceleration and deceleration delayed slightly following the corresponding changes

of photosynthesis. The following study was undertaken to determine by other methods whether respiration by these two species appeared greater in light than in darkness.

CO_2 UPTAKE VS. LIGHT INTENSITY AND CO_2 CONCENTRATION

Analysis of the effects of light intensity and CO_2 concentration on CO_2 uptake by a pteridophyte *(Selliguea caudiforme)*, a gymnosperm *(Ginkgo biloba)*, and six widely diverse angiosperms *(Fraxinus americana, Liriodendron tulipifera, Citrus paradisi, Digitalis* sp., *Pelargonium* sp., and *Euphorbia pulcherrima)* has indicated that respiration was faster in light than in darkness.[2] An essentially similar technique was used in the present studies.

A eucalyptus leaf was sealed in the chamber, illuminated at 175 fc, and left for 30 minutes. Duplicate measurements were made of CO_2 uptake by timing the fall of CO_2 concentration from 0.594 to 0.486 mgm per l, with the mean fixed at 0.540 mgm per l (300 ppm). Next the light compensation point was determined by adding light screens (sheets of white bond paper) until CO_2 concentration remained constant within the same range. Only a single observation of the compensation point was made, but it was checked by observing the slow upward and downward drifts with one more and one less sheet of paper. Then the chamber was darkened, and after a wait of at least 10 minutes duplicate measurements were made of CO_2 evolution rate in the dark by timing the rise of concentration over the same range. The series of measurements was repeated with five other eucalyptus plants. The procedure was repeated with six cottonwood leaves.

Separate analyses of variance were made for CO_2 uptake and evolution, and confidence ranges (t x standard error of mean) were computed from error terms (plant-duplicate interaction). No confidence range was computed for the light compensation point because observations were not replicated and separation of error variance from plant variance was not possible.

Results are summarized in Table I. The fact that y intercepts (a) are less than corresponding values for CO_2 evolution in darkness suggests that respiration was more rapid in light than in darkness.[2]

TABLE I

CO_2 uptake in $\mu g/sec/dm^2$ at 175 fc and 300 ppm CO_2 (CU); light compensation point in footcandles (LCP); y intercept for curve of uptake vs. light intensity (a); CO_2 evolution in $\mu g/sec/dm^2$ in darkness at 300 ppm (CE).

	CU	LCP	a	CE
Eucalyptus	0.594 ± 0.013*	34.5	0.146	0.374 ± 0.007*
Cottonwood	0.430 ± 0.075*	71.5	0.239	0.574 ± 0.075*

*1 per cent *tse* (t x standard error of mean)

Studies of the effect of CO_2 concentration on CO_2 uptake and evolution were made using eight eucalyptus leaves. Each leaf was sealed in the chamber and left for 30 minutes at 29° and 2200 fc. Uptake was timed over a short interval with the midpoint at 100 ppm. Concentration was allowed to fall to the compensation point. CO_2 was added, and the measurements were repeated twice. The chamber was darkened, and triplicate measurements were made of CO_2 evolution rate over short intervals with midpoints at 15.8, 100, and 300 ppm. The leaf was removed, and its area was measured (computed from the weight of a piece of aluminum foil cut to the pattern of the leaf).

Results are summarized in Table II. The y intercept value (a') is an estimate of the lower limit for respiration rate at 2200 fc. The fact that it greatly exceeds the comparable CO_2 evolution rates in darkness indicates that respiration was more rapid in light than in darkness.[2] This inference is valid only if respiration was not greatly accelerated by decreased CO_2 concentration. An earlier study[1] indicated that the effect was not great, and Table II provides a quantitative evaluation.

TABLE II

Effect of CO_2 concentration on CO_2 uptake and evolution by eucalyptus leaves. Uptake in $\mu g/sec/dm^2$ at 2200 fc and 100 ppm (CU); CO_2 compensation point in ppm (CCP); y intercept for curve of uptake vs. CO_2 concentration (a'); evolution in $\mu g/sec/dm^2$ at 15.8 ppm (CE_1), at 100 ppm (CE_2), and at 300 ppm (CE_3).

CU	CCP	a'	CE_1	CE_2	CE_3
0.746 ±0.013*	50.58 ±2.69*	0.764	0.446 ±0.015	0.393 ±0.015*	0.354 ±0.015*

*1 per cent *tse*

DISCUSSION

In view of the fact that respiration appears to increase with illumination, it seems likely that the surges at the beginning of light and dark periods resulted from lags between changes of rates of photosynthesis and respiration. The following sequence of events is suggested. A leaf is respiring at the usual rate in the dark. When the light is turned on, photosynthesis begins and accelerates quickly, which results in a momentarily rapid uptake of CO_2. Then, as respiration accelerates, CO_2 uptake decreases to the usual level for apparent photosynthesis. When the light is turned off, photosynthesis decelerates more quickly than does respiration, which results in a momentarily rapid but rapidly decelerating evolution of CO_2.

The large reduction of outsurge when the period of illumination was shortened to 5 seconds suggests that acceleration of respiration was delayed about that length of time. The fact that insurge appeared after only 1 second of darkness suggests that deceleration of respiration was appreciable within 1 second of darkening.

REFERENCES

1. J. P. Decker, "A rapid, post-illumination deceleration of respiration in green leaves." *Plant Physiol.* 30: 82-84, 1955.
2. ——"Further evidence of increased carbon dioxide production accompanying photosynthesis." *J. Solar Energy Sci. Eng.* 1: 30-33, 1957.
3. H. Gaffron and J. Rosenberg, "Über Rückreaktionen bei der Photosynthese." *Naturwiss.* 42: 354-364, 1955.
4. B. Kok and C. J. P. Spruit, "High initial rates of gas-exchange in respiration and photosynthesis of *Chlorella*." *Biochim. Biophys. Acta.* 19: 212-223, 1956.
5. E. I. Rabinowitch, *Photosynthesis and related processes*, II, 2. N.Y., Interscience Publishers, Inc., 1956. p. 1334-55.

SOLAR ABSTRACTS

This section brings to the attention of our readers some of the important books and papers on solar energy which have been published elsewhere during the past few months. Wherever possible, authors' abstracts have been used; other abstracts are from the standard abstract journals or are by the editorial staff of the *Journal*. Photocopies of papers abstracted below may be obtained at cost (10¢ per page) by members of the Association for Applied Solar Energy, from the Association's library at Phoenix.

• • •

Association for Applied Solar Energy, *Living with the sun, volume 1: Sixty plans selected from the entries in the 1957 International Architectural Competition to Design a Solar-Heated Residence*. Phoenix, Ariz., 1958. xii, 60 p. Illus.

The architect's original drawings for 60 of the solar house plans entered in the 1957 AFASE competition are here reproduced in a 14-in. square format. Perspective, floor plan, plot plan, and elevations are shown for each entry, accompanied by brief notes on unusual or interesting features, based on the architect's own descriptive material and the comments of the judges. The introductory section includes a preface by James M. Hunter, professional advisor for the competition, a survey of the scope and requirements of the competition, and some general remarks on the use of solar energy for space heating. Purpose of the book is to bring to the attention of architects, contractors, and home-owners the diversity of house designs which can be adapted to solar energy utilization.

• • •

Davis, Chester P., Jr. and Lipper, Ralph I., "Sun energy assistance for air-type heat pumps." *Heat. Pip. Air Cond.* 29(12): 123-28, Dec. 1957. Illus.

Acceptance of the air-type heat pump as a means of year-round air conditioning is delayed and limited by its decreased capacity when maximum capacity is required. A means of supplementing the capacity is the use of solar energy. This study does not cover the direct use of solar energy for the purpose but rather is concerned with using a heat storage with a simple low-cost flat-plate collector to capture the sun's energy. This heat is then made available for home heating via the heat pump cycle. Such a collector is described and illustrated. The study was conducted making use of two comparable independent systems with one arranged to accommodate this collector and storage.

A collector and suitable storage means can be accomplished with minimum system addition and change. Reduction and simplification of the coil defrost problem is demonstrated. This type of supplementation of heat pump capacity offers enough advantage to warrant continued development. The paper is thus a progress report on a continuing project. (authors' abst.)

• • •

Drummond, A. J. and Vowinckel, E., "The distribution of solar radiation throughout southern Africa." *J. Meteor.* 14(4): 343-53, Aug. 1957. Illus.

Since about 1950, considerable emphasis has been placed upon the registration of solar radiation in Africa by a number of the meteorological services of the territories on the continent. It is now considered that sufficient data have been assembled, with the earlier series of measurements available, to permit undertaking of the first cartographical presentation of the total shortwave radiation incomes over southern Africa. Unfortunately there is, at present, insufficient material to allow the maps to be extended northward of the equator. Twenty-three series have been used in the construction of summer and winter seasonal maps; computed values at seven other locations were employed to improve the presentation.

The seasonal areal distributions of the solar radiation, on a horizontal surface, are compared with those for the continental United States for the corresponding summer and winter periods. At ten of the stations forwarding data regularly to the World Meteorological Organization radiation center at Pretoria, records of the diffuse sky component are separately available. With the derived, average indirect fluxes for Brukkaros — the old Smithsonian Institution station in South-West Africa — these measurements constitute the densest network of its kind anywhere. The general results are discussed. (authors' abst.)

• • •

Dumortier, Jean, "Etude du rayonnement solaire, comme appoint au chauffage des bâtiments habités." (Study of solar radiation as a contribution to domestic heating.) *Flamme et Thermique* 10(108): 11-39, Sept. 1957. *Ibid.* 10(109): 13-36, Oct. 1957. Illus.

A study of the intensity of solar radiation, as a factor in the amount of energy needed to heat or to cool a house. In the first part an expression is given for the amount of solar heat absorbed by a wall. The second part deals with the determination of the various factors entering into the expression for the absorbed heat, i.e., the angle of incidence of the radiation on the wall, the insolation time, the intensity of incident solar radiation, and the energy absorbed by the wall. The practical consequences of the foregoing study are considered in the third part, in which are discussed the various corrections which must be applied for altitude, atmospheric pressure, water vapor, etc.

• • •

Farber, E. A.; Bussell, W. H., and Bennett, J. D., "Solar energy used to supply service hot water." *Air Cond. Heat. Vent.* 54(10): 75-79, Oct. 1957. Illus.

Data are presented of interest to the designer of a system that uses solar energy for heating water. Figures are given as to the availability of sunshine in the United States, what can be expected from a good solar water heating installation, the effect of multiple glass covers on the absorber, heat losses, how much energy the water can be expected to absorb, and a comparison of the costs of heating water by solar energy, gas, and electricity. (authors' abst.)

• • •

Halsted, R. E., "Temperature consideration in solar battery development." *J. App. Phys.* 28(10): 1131, Oct. 1957. Illus.

Semiconductor materials of band gap appreciably greater than that of silicon may prove useful for photovoltaic solar energy converters operating at elevated temperatures. Such operation is of interest for applications where solar energy concentration can be employed to reduce the photovoltaic surface area required to produce a desired amount of electrical power. (authors' abst.)

• • •

Khanna, Mohan L., "Concentration of palm juice with solar energy." *J. Sci. Ind. Res.* 16A(6): 269-70, 1957.

A multi-reflector type of concentrator with 9 plane-mirror

reflectors arranged in a semicircle has been used by the National Physical Laboratory of India to concentrate solar heat for evaporating palm juice. Results are given for experiments in which palm juice was concentrated by direct solar heating and with the help of the concentrator. Results are also given for five field trials on the evaporation of palm juice conducted at the Palm Gur Technological Institute, Dhanu.

* * *

Kondrat'ev, K. Ia., *Luchistaia energiia solntsa.* (Radiant energy of the sun.) Ed. by P. N. Tverskoi. Leningrad, Gidrometizdat., 1954. 599 p. Illus.

The first part of this comprehensive book on solar radiation follows the lines of Kalitin's classic text of 1938, though incorporating findings through 1953. The last part of the book is completely original and based almost entirely on recent data and literature from Russia and abroad. The systematically arranged chapters cover: (1)General concepts of radiation; (2) Theory of actinometry of short (and visible) wave radiation in the atmosphere; (3) extinction in atmosphere due to scattering; (4) atmospheric extinction due to absorption; (5) General extinction, transmissivity, effects of clouds, geographical variation; (6) spectral distribution of solar and transmitted energy; (7) flux and total heat of direct solar radiation; (8) reflected radiation; (9) albedo of surface of earth and clouds; (10) global radiation; (11) insolation under special conditions (vegetation, forests, water, snow, ice); (12) applications. The book is profusely illustrated with graphs and the text supported by selected tabular data, theory, and extensive references on every subject (arranged by chapters). Although a good percentage of the reference material is from foreign sources, the tables have mostly been given in Cyrillic (Russian). The subject index gives a good idea of the wide variety of instrumental, observational, and theoretical subjects covered. *(Meteor. Absts.)*

* * *

Linder, E. G., "Solar batteries." (In: *Ten years of progress: proceedings, Tenth Annual Battery Research and Development Conference, May 23, 1956.* Power Sources Div., Signal Corps Engineering Labs., Fort Monmouth, N. J., PB 125427. p. 59-62. Illus.

The origin and early development of photovoltaic cells from 1839 to the present day is reviewed, and the operation of the p-n type solar cell is described. Recent work with solar batteries, since 1954, at the Bell Telephone Labs, the General Electric Company, and the Wright Air Development Center is reviewed. The cost of commercial batteries is considered.

* * *

Morse, R. N., "Solar water heaters for domestic and farm use." *Commonwealth Scientific and Industrial Research Organization, Eng. Sect., Rept.* ED 5, Sept. 1957. 15+p. Illus.

A solar water heater is described having an output of 48 gal of hot water per day suitable for domestic or farm use. Complete details in the form of drawings, material lists, and photographs are included, together with an account of the problems met in actual installations. Performance and operating costs under Melbourne conditions are discussed briefly.

The present report combines Rept. E.D. 3 dated July 1956, and Supplement dated June, 1957, and largely supersedes *C.S.I.R.O. Central Exp. Workshops Rept.* E.D. 1 — "The design and construction of solar water heaters" by R. N. Morse: April 1954; rev. ed. Feb. 1955. (author's abst.)

* * *

Noguchi, Tetsuo; Mizuno, Masao, and Noguchi, Choji, "High temperature research in a solar furnace. I. On the fusion of metal oxides." *Rept. Govt. Ind. Res. Inst. Nagoya.* 6(11): 663, Nov. 1957.

The solar furnace having a 2-m diameter aluminum reflector, whose energy concentration in the focal plane was estimated in a previous paper to be about 300 watts per sq cm, is being used in the fusion study of metal oxides. Some improvements have been made in the sample holder so as to permit continuous melting, and a blackbody container has been attached to the holder in order to elevate the attainable temperature during the heat treatment of a sample in air.

This paper also correlates the results of fusion of the mono- and binary systems of metal oxides, such as BeO, CaO, MgO, ZrO_2, $ZrSiO_4$, Al_2O_3, and TiO_2; Al_2O_3-TiO_2, SiO_2-TiO_2, MgO-TiO_2, Al_2O_3-ZnO, and MgO-Cr_2O_3. Most of the specimens were fused into molten masses and were then inspected through a microscope; $ZrSiO_4$ is decomposed into ZrO_2 and SiO_2. In the binary systems of Al_2O_3-TiO_2, Al_2O_3-ZnO, and MgO-Cr_2O_3, the crystals of β-Al_2TiO_5, ZnO·Al_2O_3 and MgO·Cr_2O_3 are observed respectively, and the formation of any compounds is not found in the systems of SiO_2-TiO_2 and MgO-TiO_2. (authors' abst.)

* * *

Olgyay and Olgyay, *Solar control & shading devices.* Princeton, N. J., Princeton University Pr., 1957. 201 p. Illus.

Previously known architectural principles of solar analysis and control are reviewed, and the authors' own research in this field is described. The first section discusses the role of shading devices as architectural elements, the technical considerations in the design of solar protection, and the practical applications of shading methods. The last part of the book contains over 100 examples of solar-control devices in existing buildings, illustrated and evaluated.

* * *

Sihvonen, Y. T., "Spectroheliometer for continuously monitoring solar radiation in five wavelength bands." *Rev. Sci. Instr.* 28(8): 628-34, Aug. 1957. Illus.

An instrument that quantitatively records and integrates solar radiation has been developed and put into operation. This instrument, called a spectroheliometer, records and integrates automatically from sunrise to sunset. Total radiation is measured in addition to sampling radiation in 5 distinct spectral regions: 3095-3260 A, 3410-3630 A, 3865-4150 A, 4420-4900 A, and 5385-6295 A. Solar power in these bands as low as 10^{-5} watt per sq cm has been quantitively measured. The band widths intercepted are accurate to $\pm$ 15 A with an estimated $\pm$ 5 to 8 per cent maximum error in determining absolute solar power and energy. (author's abst.)

* * *

Threlkeld, J. L. and Jordan R. C., "Direct solar radiation available on clear days." *Heat Pip. Air Cond.* 29(12): 135-45, Dec. 1957. Illus.

This paper presents the results of research on the incidence of direct solar radiation during clear days in the United States. A fundamental procedure for determining atmospheric transmission factors for various atmospheric conditions and for various elevations is presented. A more approximate procedure involving the concept of a basic atmosphere together with atmospheric clearness numbers is also presented. Correlations with observed solar radiation at several localities are included. (authors' abst.)

* * *

Trombe, F. and Foex, M., "Dispositif permettant la culture dans des régions arides et ensoleillées." (Apparatus to assist plant cultivation in arid and sunny regions.) *Procès-verbal Acad. Agric. France,* Oct. 30, 1957. 3 p.

An apparatus has been developed at the Laboratoire de l'Energie Solaire in Mont Louis to aid in the cultivation of plants in sunny, arid regions where only saline water is available. The apparatus consists of a series of enclosures for the growing plants which allows entry of sunlight through a transparent, inclined glass or plastic roof. Inside the enclosure, pans of saline water are fixed above the level of the vegetation. This water is evaporated by the sunlight, condenses on the transparent cover, and runs down to the level of the soil.

In a series of tests run at Mont Louis with an experimental apparatus of this type, green beans were grown during 2 months of the summer.